EUROPEAN ORGANIZATION FOR NUCLEAR RESEARCH (CERN)

CERN-EP-2025-029
2025/04/14

CMS-TOP-22-011

Search for charged-lepton flavour violation in top quark interactions with an up-type quark, a muon, and a τ lepton in proton-proton collisions at $\sqrt{s} = 13\,\text{TeV}$

The CMS Collaboration*

Abstract

A search for charged-lepton flavour violation (CLFV) in top quark (t) production and decay is presented. The search uses proton-proton collision data corresponding to $138\,\text{fb}^{-1}$ collected with the CMS experiment at $\sqrt{s} = 13\,\text{TeV}$. The signal consists of the production of a single top quark via a CLFV interaction or top quark pair production followed by a CLFV decay. The analysis selects events containing a pair of oppositely charged muon and hadronically decaying τ lepton and at least three jets, where one has been identified to originate from the fragmentation of a bottom quark. Machine learning classification techniques are used to distinguish signal from standard model background events. The results of this search are consistent with the standard model expectations. The upper limits at 95% confidence level on the branching fraction $\mathcal{B}$ for CLFV top quark decays to a muon, a τ lepton, and an up or a charm quark are set at $\mathcal{B}(\text{t} \to \mu\tau\text{u}) < (0.040, 0.078, \text{and } 0.118) \times 10^{-6}$, and $\mathcal{B}(\text{t} \to \mu\tau\text{c}) < (0.810, 1.710, \text{and } 2.052) \times 10^{-6}$ for scalar, vector, and tensor-like operators, respectively.

Submitted to the Journal of High Energy Physics

*See Appendix A for the list of collaboration members

1 Introduction

The standard model (SM) of particle physics successfully describes the properties of all elementary particles and their interactions with a small number of free parameters, but it is known to be incomplete. Extensions of the SM aim to describe several phenomena such as dark matter [1–4] and the baryon asymmetry of the universe [5].

The observation of neutrino oscillations [6] confirms a non-zero neutrino mass and neutral-lepton flavour violation. The existence of neutrino mass terms implies charged-lepton flavour violation (CLFV) in the SM at the loop level. An example is the CLFV branching fraction $\mathcal{B}$ of a muon decay into an electron and a photon, which is of the order of 10^{-55} in the SM, whereas extensions of the SM predict branching fractions as high as 10^{-4} [7]. The observation of CLFV would be a decisive signature of physics beyond the SM.

Recent combinations of measured ratios of B meson decays into D and D* mesons [8] are in tension with the corresponding SM predictions. This has sparked interest in models that aim to explain these deviations, and at the same time introduce a new source of lepton flavour violation (LFV) effects. For example, leptoquark models developed to explain the anomalies in the b quark sector could generate a four-fermion interaction that would allow the $\mathrm{t} \to \mathrm{c}\ell_i\ell_j$ decay at tree level [9], where ℓ denotes a charged lepton and the indices i and j denote the flavour. Recently, the LHCb Collaboration reported a 1.9 standard deviation difference from the SM predictions of these ratios [10]. Although the new measurement aligns more closely with the SM expectations, the interest in the search for LFV remains.

The ATLAS Collaboration has performed a search for CLFV in $\mu\tau\mathrm{qt}$ interactions using proton-proton (pp) collision data corresponding to $140\,\mathrm{fb}^{-1}$ at $\sqrt{s} = 13\,\mathrm{TeV}$ [11]. Events with two muons, one hadronically decaying τ lepton (τ_h), and at least one jet identified to originate from the fragmentation of a b quark (b jet) are analysed, resulting in an upper limit at 95% confidence level (CL) of $\mathcal{B}(\mathrm{t} \to \mu\tau\mathrm{q}) < 8.7 \times 10^{-7}$, where q can be either a u or c quark. The CMS Collaboration has performed searches for CLFV involving $\mathrm{e}\mu\mathrm{tq}$ interactions in final states with two or three leptons [12, 13]. The upper limits at 95% CL on the corresponding branching fractions range from 10^{-6} to 10^{-8}.

A new search for CLFV involving interactions with top quarks is presented in this article. We focus on final states with a muon and a τ_h with opposite charge, and multiple jets. The analysis uses pp collision data collected with the CMS detector at $\sqrt{s} = 13\,\mathrm{TeV}$, corresponding to an integrated luminosity of $138\,\mathrm{fb}^{-1}$. The analysis focuses on CLFV single top quark (ST CLFV) production and top quark pair ($\mathrm{t\bar{t}}$) production with a subsequent CLFV decay (TT CLFV), as illustrated in Fig. 1. Signal events are modelled using an effective field theory (EFT) framework with dimension-six operators $O_a^{(6)}$ and the corresponding Wilson coefficients $C_a^{(6)}$, where the

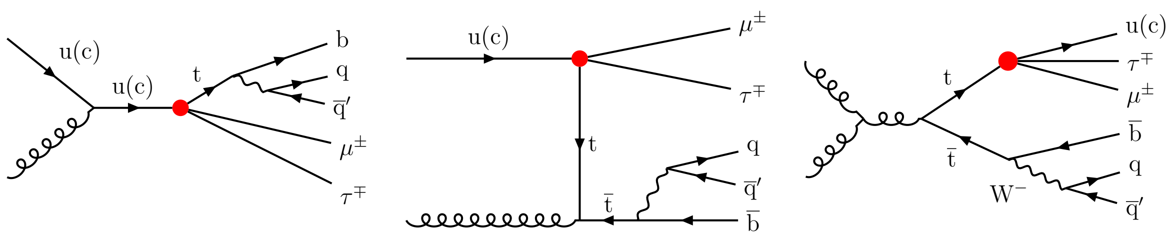

Figure 1: Example Feynman diagrams at leading order for the CLFV production of a single top quark (left and centre) and top quark pair production followed by a CLFV decay (right). Red dots indicate the effective CLFV coupling.

Table 1: The EFT operators considered in this analysis and their definition. The ε parameter is a fully asymmetric two-dimensional tensor, γ^{μ} are the Dirac matrices, and $\sigma^{\mu\nu} = \frac{i}{2}[\gamma^{\mu}, \gamma^{\nu}]$. Left-handed doublets of leptons and quarks are denoted by ℓ_i and q_k, respectively, where the indices i and k denote the lepton and quark flavours. Right-handed lepton and quark singlets are denoted by e_i and u_k, respectively.

Structure	Operator	Definition
Scalar	$O_{\ell \mathrm{equ}}^{1(ijkl)}$	$(\bar{\ell}_i \mathrm{e}_j)\varepsilon(\bar{\mathrm{q}}_k \mathrm{u}_l)$
Vector	$O_{\ell \mathrm{q}}^{1(ijkl)}$	$(\bar{\ell}_i \gamma^{\mu} \ell_j)(\bar{\mathrm{q}}_k \gamma_{\mu} \mathrm{q}_l)$
	$O_{\ell \mathrm{u}}^{(ijkl)}$	$(\bar{\ell}_i \gamma^{\mu} \ell_j)(\bar{\mathrm{u}}_k \gamma_{\mu} \mathrm{u}_l)$
	$O_{\mathrm{eq}}^{(ijkl)}$	$(\bar{\mathrm{e}}_i \gamma^{\mu} \mathrm{e}_j)(\bar{\mathrm{q}}_k \gamma_{\mu} \mathrm{q}_l)$
	$O_{\mathrm{eu}}^{(ijkl)}$	$(\bar{\mathrm{e}}_i \gamma^{\mu} \mathrm{e}_j)(\bar{\mathrm{u}}_k \gamma_{\mu} \mathrm{u}_l)$
Tensor	$O_{\ell \mathrm{equ}}^{3(ijkl)}$	$(\bar{\ell}_i \sigma^{\mu\nu} \ell_j)\varepsilon(\bar{\mathrm{q}}_k \sigma_{\mu\nu} \mathrm{u}_l)$

generic Lagrangian is given by

$$\mathcal{L}_{\mathrm{eff}} = \mathcal{L}_{\mathrm{SM}} + \frac{1}{\Lambda^2} \sum_a C_a^{(6)} O_a^{(6)} + \mathcal{O}\left(\frac{1}{\Lambda^4}\right). \quad (1)$$

In this analysis, the $O_a^{(6)}$ are defined as linear combinations of the operators given in Table 1. The sum runs over the relevant dimension-six operators introducing CLFV effects and the new physics scale Λ is set to 1 TeV. Terms of order $1/\Lambda^4$ and higher are neglected [14, 15]. Table 1 summarizes the relevant EFT operators considered in this analysis and their grouping according to the Lorentz structure. The analysis considers six independent Wilson coefficients that lead to CLFV couplings: $C_{\mathrm{tc}\mu\tau}^{\mathrm{tensor}}$, $C_{\mathrm{tc}\mu\tau}^{\mathrm{vector}}$, $C_{\mathrm{tc}\mu\tau}^{\mathrm{scalar}}$, $C_{\mathrm{tu}\mu\tau}^{\mathrm{tensor}}$, $C_{\mathrm{tu}\mu\tau}^{\mathrm{vector}}$, $C_{\mathrm{tu}\mu\tau}^{\mathrm{scalar}}$. For each coefficient, the subscript denotes the CLFV interaction vertex and the superscript represents the Lorentz structure of the corresponding operator.

This article is organized as follows. We start with a brief overview of the CMS detector in Section 2. A detailed description of the signal and background modelling is presented in Section 3. In Section 4, we describe the physics objects and the selection requirements, followed by improvements of the background modelling in Section 5. The reconstruction of the top quarks and W bosons, as well as the signal discrimination are explained in Section 6. Systematic uncertainties that contribute to the analysis are listed in Section 7. The results of the search are presented in Section 8. We conclude with a summary in Section 9. Tabulated results are provided in the HEPData record for this analysis [16].

2 The CMS detector

The central feature of the CMS apparatus is a superconducting solenoid of 6 m internal diameter, providing a magnetic field of 3.8 T. Within the solenoid volume are a silicon pixel and strip tracker, a lead tungstate crystal electromagnetic calorimeter (ECAL), a brass and scintillator hadron calorimeter (HCAL), each composed of a barrel and two endcap sections. Forward calorimeters extend the pseudorapidity (η) coverage provided by the barrel and endcap detectors.

Events of interest are selected using a two-tiered trigger system. The first level, composed of custom hardware processors, uses information from the calorimeters and muon detectors to select events at a rate of around 100 kHz within a fixed latency of about 4 μs [17]. The second level, known as the high-level trigger, consists of a farm of processors running a version of the full event reconstruction software optimized for fast processing, and reduces the event rate to around 1 kHz before data storage [18]. A more detailed description of the CMS detector, together with a definition of the coordinate system used and the relevant kinematic variables, can be found in Ref. [19].

3 Data and simulated samples

Data events were collected with the CMS detector in pp collisions in the years 2016 to 2018 at $\sqrt{s} = 13$ TeV, corresponding to an integrated luminosity of 138 fb^{-1}. The data analysed in this search were recorded by triggers requiring the presence of a single muon. We use high-level trigger paths with isolated muons [20], where the muon transverse momentum (p_{T}) thresholds vary between 24–27 GeV, depending on the data-taking period.

Signal LFV events are generated at leading order (LO) accuracy with MADGRAPH5_aMC@NLO 2.6.5 [21], separately for single top quark and $\mathrm{t\bar{t}}$ production using the SMEFTFR model [22]. The ST CLFV cross sections are calculated at LO with MADGRAPH5_aMC@NLO. The TT CLFV signal cross sections are calculated as product of the SM $\mathrm{t\bar{t}}$ cross section of 833.9 pb as obtained from the TOP++ program at next-to-next-to-LO (NNLO) in perturbative quantum chromodynamics (QCD) including soft-gluon resummation at next-to-next-to-leading-logarithmic (NNLL) order [23] with the CLFV top quark branching fractions $\mathcal{B}$. These are obtained from the partial widths of the CLFV top quark decay from Refs. [24, 25], which do not depend on the decayed quark flavour. We use MADGRAPH5_aMC@NLO to assign weights to simulated signal events, such that the kinematic variables and normalization of the signal samples resemble the predictions from SMEFTSIM [26] as done in Ref. [13]. The event weight is computed by comparing the matrix element amplitudes of SMEFTFR and SMEFTSIM for each event. The method is validated using signal samples generated with SMEFTSIM. Table 2 summarizes the predicted cross sections for each channel considered with the Wilson coefficients set to $C_a/\Lambda^2 = 1\,\text{TeV}^{-2}$.

The top quark p_{T} spectrum in $\mathrm{t\bar{t}}$ production simulated at LO and next-to-LO (NLO) differs from higher-order theoretical predictions [27–29]. Therefore, the distribution in the top quark p_{T} in the TT CLFV events is corrected sequentially from LO to NLO and to the NNLO QCD+NLO electroweak prediction utilizing simulated SM $\mathrm{t\bar{t}}$ samples and theory predictions [30, 31], respectively.

Background processes are divided into three groups: $\mathrm{t\bar{t}}$ production, single top quark production, and the other minor backgrounds. These are referred to as "$\mathrm{t\bar{t}}$", "single t", and "other", respectively. The largest background process is SM $\mathrm{t\bar{t}}$ production in dileptonic decay channels and lepton+jets channels. It is simulated at NLO precision using POWHEG v2 [32–34]. The p_{T} spectrum in the SM $\mathrm{t\bar{t}}$ sample is corrected to match the NNLO predictions, similar to the TT CLFV signal samples. The single t background consists of t-channel and s-channel processes, and W boson associated production (tW). These are simulated at NLO accuracy using POWHEG v2, MADGRAPH5_aMC@NLO, and POWHEG v2 [35], respectively. The predicted NLO cross sections are 134 and 80 pb for t-channel top quark and antiquark production, respectively, and 6.8 pb for s-channel production [36, 37]. The tW cross section is 79.3 pb, calculated at approximate NNLO accuracy [38, 39]. Other smaller SM background contributions arise

Table 2: Predicted cross sections for CLFV signal processes are presented together with uncertainties from missing higher orders in matrix element calculations, considering operators with different Lorentz structures using $C_a/\Lambda^2 = 1\,\text{TeV}^{-2}$. The results for ST CLFV are at LO accuracy and the ones for TT CLFV are at NNLO+NNLL accuracy for the $\mathrm{t\bar{t}}$ production with LO accuracy for the CLFV decay.

Process	Lorentz structure	Cross section [fb]
ST CLFV tu$\mu\tau$	Scalar	$59.1^{+11.1}_{-8.7}$
	Vector	276^{+50}_{-39}
	Tensor	1272^{+220}_{-180}
ST CLFV tc$\mu\tau$	Scalar	$3.74^{+0.63}_{-0.54}$
	Vector	$19.5^{+3.1}_{-2.6}$
	Tensor	96^{+14}_{-12}
TT CLFV tq$\mu\tau$	Scalar	$2.69^{+0.71}_{-0.53}$
	Vector	$21.5^{+5.7}_{-4.2}$
	Tensor	129^{+34}_{-25}

from $\mathrm{t\bar{t}}$ production in fully hadronic decays, $\mathrm{t\bar{t}}$ production in association with a vector boson ($\mathrm{t\bar{t}Z}$ and $\mathrm{t\bar{t}W}$) or a Higgs boson ($\mathrm{t\bar{t}H}$), simulated with MADGRAPH5_aMC@NLO and POWHEG v2 at NLO accuracy, respectively, Drell–Yan and W boson production, simulated with MADGRAPH5_aMC@NLO at LO with up to 4 additional jets using MLM matching [40], and diboson (WW, WZ, and ZZ) processes generated with PYTHIA 8.240 [41] at LO accuracy. A top quark mass of 172.5 GeV is used in all simulated samples. The parton distribution function (PDF) set used for the event generation is NNLO NNPDF 3.1 [42], while PYTHIA with the CP5 tune [43] is used to simulate initial- and final-state radiation, the parton shower, and the hadronization process. All simulated samples are interfaced to GEANT4 [44] for a detailed simulation of the CMS detector response.

Additional pp interactions within the same or nearby bunch crossings (pileup) are simulated by generating inelastic pp events using PYTHIA with a total inelastic cross section of 69.2 mb [45]. These are superimposed on the hard-scattering events. The generated number of pp interactions is corrected such that the simulated distribution in the number of primary vertices matches that observed in the data.

4 Object reconstruction and event selection

The particle-flow (PF) algorithm [46] aims to reconstruct and identify each individual particle in an event, with an optimized combination of information from the various elements of the CMS detector including charged-particle tracks from the tracking detector, energy deposits in the HCAL and ECAL, and reconstructed tracks from the muon chambers. Particles in each event are reconstructed and identified as either electrons, muons, photons, charged hadrons, or neutral hadrons. The primary vertex is taken to be the vertex corresponding to the hardest scattering in the event, evaluated using tracking information alone, as described in Section 9.4.1 of Ref. [47].

Muons are identified as tracks in the central tracker consistent with either a track or several hits in the muon system, and associated with calorimeter deposits compatible with the muon hypothesis. The energy of muons is obtained from the curvature of the corresponding track. Muons are required to have $p_{\mathrm{T}} > 50\,\mathrm{GeV}$ and $|\eta| < 2.4$. Moreover, muons need to be isolated and pass the "tight" identification criteria, which corresponds to an efficiency of 96% [20]. The muons passing "loose" isolation and identification criteria are used to veto events with additional muons with $p_{\mathrm{T}} > 15\,\mathrm{GeV}$.

Electrons are identified as a primary charged-particle track and potentially multiple ECAL energy clusters corresponding to the extrapolation of this track to the ECAL and to possible bremsstrahlung photons emitted along the way. The electron momentum is estimated by combining the energy measurement in the ECAL with the momentum measurement in the tracker. Only electrons passing the "veto" cut-based identification [48] with $p_{\mathrm{T}} > 15\,\mathrm{GeV}$ and $|\eta| < 2.4$ are considered as these are used to reject events with additional leptons.

Charged hadrons are identified as charged-particle tracks that are neither identified as electrons nor muons. Finally, neutral hadrons are identified as HCAL energy clusters not linked to any charged-hadron trajectory, or as a combined ECAL and HCAL energy excess with respect to the expected charged-hadron energy deposit. The energy of charged hadrons is determined from a combination of their momentum measured in the tracker and the matching ECAL and HCAL energy deposits, corrected for the response function of the calorimeters to hadronic showers. The energy of neutral hadrons is obtained from the corresponding corrected ECAL and HCAL energy deposits.

The PF candidates are clustered into jets using the anti-k_{T} clustering algorithm [49] with a distance parameter of 0.4, implemented in the FASTJET package [50, 51]. The jet momentum is determined as the vectorial sum of all particle momenta in the jet, and is found from simulation to be, on average, within 5–10% of the true momentum over the entire p_{T} spectrum and detector acceptance. Pileup can contribute additional tracks and calorimetric energy depositions to the jet momentum. To mitigate this effect, tracks identified as originating from pileup vertices are discarded and a correction is applied for the remaining contributions. Jet energy corrections are derived from simulation studies so that the average measured energy of reconstructed jets becomes identical to that of particle-level jets. In situ measurements of the momentum balance in dijet, photon+jet, Z+jet, and multijet events are used to determine any residual differences between the jet energy scale (JES) in data and in simulation, and appropriate corrections are made [52]. The jet energy resolution (JER) amounts typically to 15–20% at 30 GeV, 10% at 100 GeV, and 5% at 1 TeV [52]. Heavy-flavour jets are identified based on the DEEPJET algorithm [53–55] at the medium working point defined by a light-quark or gluon jet misidentification rate of 1%, resulting in a b jet identification efficiency of 75%. Only jets with $p_{\mathrm{T}} > 40\,\mathrm{GeV}$ and $|\eta| < 2.4$ are considered.

Hadronic τ lepton decays are reconstructed from jets, using the hadrons-plus-strips algorithm [56], which combines one or three tracks with energy deposits in the calorimeters, to identify the τ_{h} lepton decay modes. Neutral pions are reconstructed as strips with dynamic size in η-ϕ, with ϕ denoting the azimuthal angle in radians, from reconstructed electrons and photons [48]. The strip size varies as a function of the p_{T} of the electron or photon candidate. To distinguish genuine τ_{h} decays from jets originating from the hadronization of quarks or gluons, and from electrons or muons, the DEEPTAU algorithm is used [57]. Information from all individual reconstructed particles near the τ_{h} axis is combined with properties of the τ_{h} candidate and the event. The τ_{h} are required to pass kinematic requirements of $p_{\mathrm{T}} > 40\,\mathrm{GeV}$ and $|\eta| < 2.3$. Candidates are selected using the "very tight" criteria to discriminate against quark and gluon jets, and the "tight" and "very loose" criteria against muons and electrons, respectively. The chosen identification working points have τ_h average efficiencies of about 50, 98, and 98.8% with misidentification probabilities of about 0.4, 2, and 0.02% for the discrimination against jets, electrons, and muons, respectively [57]. The rate of a jet to be misidentified as τ_h by the DEEPTAU algorithm depends on the p_T and quark flavour of the jet. The τ_h energy scale corrections are derived from a binned maximum likelihood fit of the distributions of observables sensitive to the energy shift [56, 57].

The missing transverse momentum vector $\vec{p}_\mathrm{T}^\mathrm{miss}$ is computed as the negative vector p_T sum of all the PF candidates in an event, and its magnitude is denoted as $p_\mathrm{T}^\mathrm{miss}$ [58]. The $\vec{p}_\mathrm{T}^\mathrm{miss}$ is modified to account for corrections to the energy scale of the reconstructed jets in the event.

The event selection is designed to isolate final-state particles characteristic of CLFV signal processes in both single top quark and top quark pair production. Events are selected via a sequence of requirements on selected physics objects. Events must have exactly one tight muon with no additional muons or electrons. Furthermore, events with exactly one τ_h candidate are selected, separated by $\Delta R > 0.4$ from the muon. The angular distance ΔR is defined as $\Delta R = \sqrt{(\Delta\eta)^2 + (\Delta\phi)^2}$, where $\Delta\eta$ and $\Delta\phi$ are the differences in pseudorapidity and azimuthal angle between the τ_h and muon candidates, respectively. Only events containing an oppositely charged muon-τ_h pair are considered. We remove jets with $\Delta R < 0.4$ from the selected muon and τ_h candidates. Events must contain at least three jets, where exactly one jet must be a b jet.

The lepton identification efficiencies for the muon and τ_h candidates used in this analysis are measured using the "tag-and-probe" technique [59]. Efficiency differences between data and simulation are corrected for by applying scale factors (SFs) to the simulation.

5 Background from jets misidentified as τ_h

Despite the discrimination power of the DEEPTAU algorithm with a τ_h misidentification probability of less than 1% for quark and gluon jets, a non-negligible background contribution remains from events with misidentified τ_h candidates. Most of these are $\mathrm{t\bar{t}}$ events in the lepton+jets decay channel, where the correctly identified muon originates from the top quark decay chain $\mathrm{t} \to \mathrm{Wb} \to \mu\nu\mathrm{b}$. Other events with a misidentified τ_h candidate originate from W+jet and single t production. Because of the much smaller muon misidentification rate, events with a misidentified muon and a genuine τ_h candidate are negligible compared to events with a misidentified τ_h candidate. The rate of misidentified τ_h candidates is not well modelled by simulation, therefore an approach based on CRs in data is used to calculate the contribution of events with a misidentified τ_h candidate in this analysis.

The "ABCD method", as introduced in Ref. [60], uses additional event categories to calculate scaling factors for simulated events to correct for a mismodelling in the simulation. The signal region (SR) D contains events that pass all selections of Section 4, with muon and τ_h candidates having opposite charges. An inversion of the charge requirement defines CR B, where the muon and τ_h candidates have the same charge. Additional CRs are constructed by requiring events to have a τ_h candidate passing the "loose", but failing the "very tight" requirement of the τ_h discrimination against jets. These events enter CR A if the muon and τ_h candidates have the same charge, and CR C if they have opposite charges. The same requirements on the jet and b jet multiplicities are applied to all regions. The number of events with a misidentified τ_h candidate in SR D, $N^\mathrm{D}_\text{mis-ID}$, is calculated from data in CRs A, B, and C, as

$$N^\mathrm{D}_\text{mis-ID} = N^\mathrm{C}\frac{N^\mathrm{B}}{N^\mathrm{A}}. \quad (2)$$

In each region i, the number of events N^i entering Eq. (2) is the number of observed events in data N^i_{obs} corrected by the number of events with a genuine τ_h lepton N^i_{genuine},

$$N^i = N^i_{\mathrm{obs}} - N^i_{\mathrm{genuine}}. \qquad (3)$$

The value of N^i_{genuine} is determined using generator-level information in simulated events, which contains the properties of particles as defined by the event generator before the detector simulation. The ABCD method corrects the normalization of simulated background processes with misidentified τ_h candidates in the SR D under the assumption that the ratio between the number of jets misidentified as τ_h passing the "very tight" and "loose" selection criteria is the same for same-sign and opposite-sign events. The SF applied to simulated background events is calculated as $N^{\mathrm{D}}_{\text{mis-ID}}/(N^{\mathrm{D}}_{\text{tot. bkg.}} - N^{\mathrm{D}}_{\mathrm{genuine}})$, where $N^{\mathrm{D}}_{\text{tot. bkg.}}$ is the number of all simulated background events in SR D. This SF is calculated and applied separately for each data-taking period and τ_h decay mode.

We show distributions of important event properties in Fig. 2, after the event selection described in Section 4. Distributions obtained from data are compared to distributions from the sum of all SM background processes, including the SFs from the ABCD method. The signal processes are normalized to the total number of events observed in data for visibility of histograms.

The total number of expected events for CLFV signal and background processes, where the background yields include τ_h misidentification SFs from the ABCD method, are presented in Table 3 and compared to data.

6 Discrimination of signal and background

6.1 Reconstruction of top quark and W boson

In both ST CLFV and TT CLFV signal events, a top quark is produced that decays hadronically through the decay chain $\mathrm{t} \to \mathrm{bW} \to \mathrm{bq\overline{q}'}$. Background events mostly originate from $\mathrm{t\bar{t}}$ production consisting of 79.7% from the dileptonic decay channel and 9.3% from the lepton+jets decay channel after the background estimation.

To benefit from this difference, the hadronic top quark decay is reconstructed using a χ^2 method. The χ^2 variable is constructed as

$$\chi^2 = \left(\frac{m_\mathrm{t} - m_{\mathrm{bjj'}}}{\sigma_\mathrm{t}}\right)^2 + \left(\frac{m_\mathrm{W} - m_{\mathrm{jj'}}}{\sigma_\mathrm{W}}\right)^2, \qquad (4)$$

with the expected mass values $m_\mathrm{t} = 173.95\,\mathrm{GeV}$ and $m_\mathrm{W} = 84.2\,\mathrm{GeV}$, and resolutions $\sigma_\mathrm{t} = 17.07\,\mathrm{GeV}$ and $\sigma_\mathrm{W} = 9.91\,\mathrm{GeV}$. The mass and resolution values are computed in simulated $\mathrm{t\bar{t}}$ events from detector-level jets matched to generator-level jets from the top quark and W boson decays. The χ^2 is calculated for all possible combinations of non-b-tagged jets in an event. The reconstructed W boson candidate is formed by two jets with mass $m_{\mathrm{jj'}}$ and the selected b-tagged jet is assigned to the reconstructed top quark candidate with mass $m_{\mathrm{bjj'}}$. For each event, the reconstruction hypothesis is chosen that results in the smallest value of χ^2.

The results of the reconstruction are presented in Fig. 3 for data, simulated signal and background events. The SFs from the ABCD method are applied to the background simulation. Distributions in signal events show more pronounced peaks around m_t and m_W in the reconstructed top quark and W boson masses, respectively, than the background distributions. The

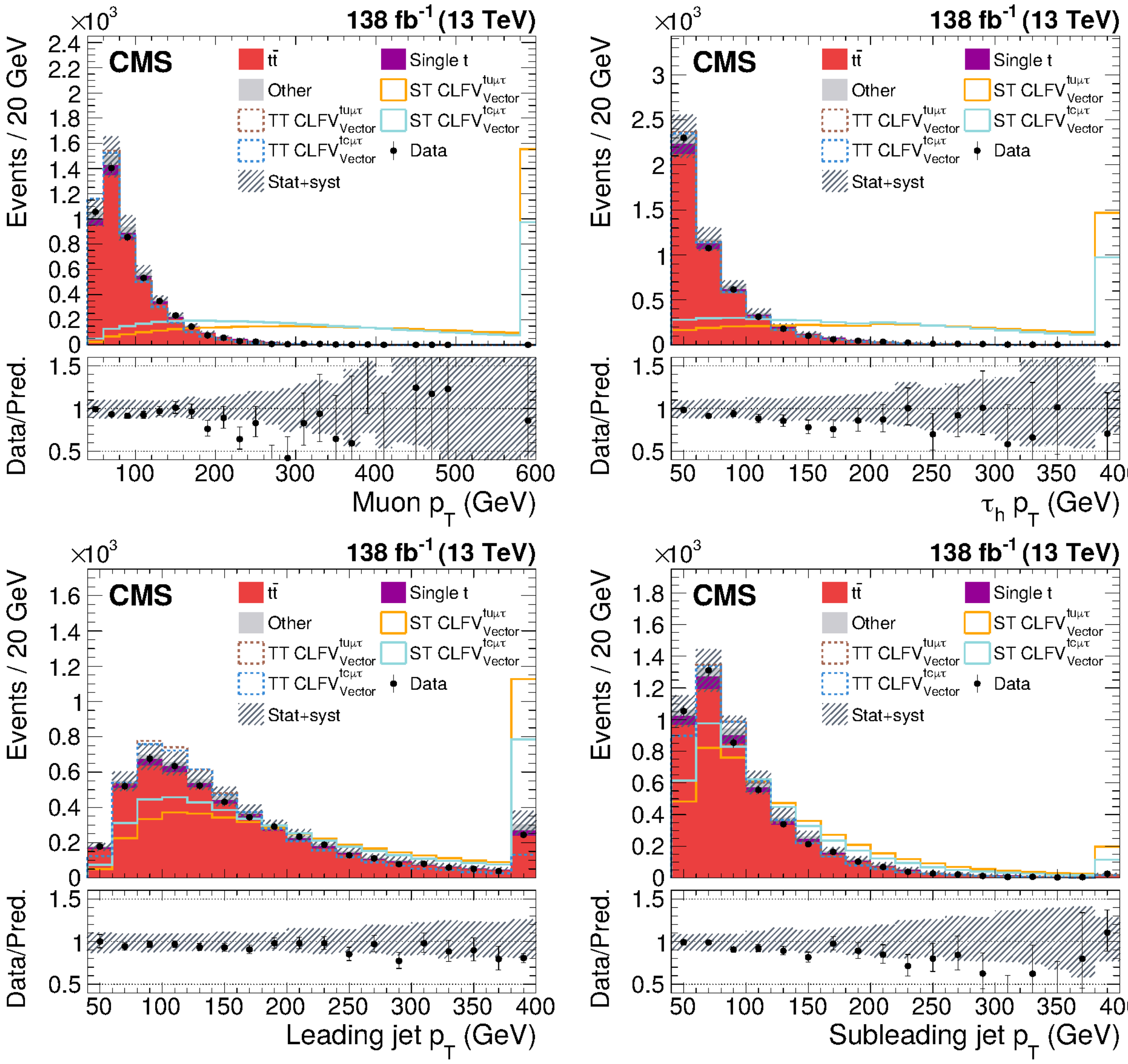

Figure 2: Distributions in p_T of the muon (upper left), τ_h (upper right), p_T-leading jet (lower left), and p_T-subleading jet (lower right) after all selection steps. The solid and dashed lines show the signal distributions, individually for each type of operator and interaction for the vector Lorentz structure as an example. The signals are normalized to the total number of events in data for visibility. The last bin in each histogram contains the overflow. The color filled histograms show the stacked background contributions. The data are shown as filled points. The shaded band displays the total uncertainty in the predicted SM background, consisting of statistical and systematic uncertainties added in quadrature. The panels below the distributions show the ratio of data to the background prediction.

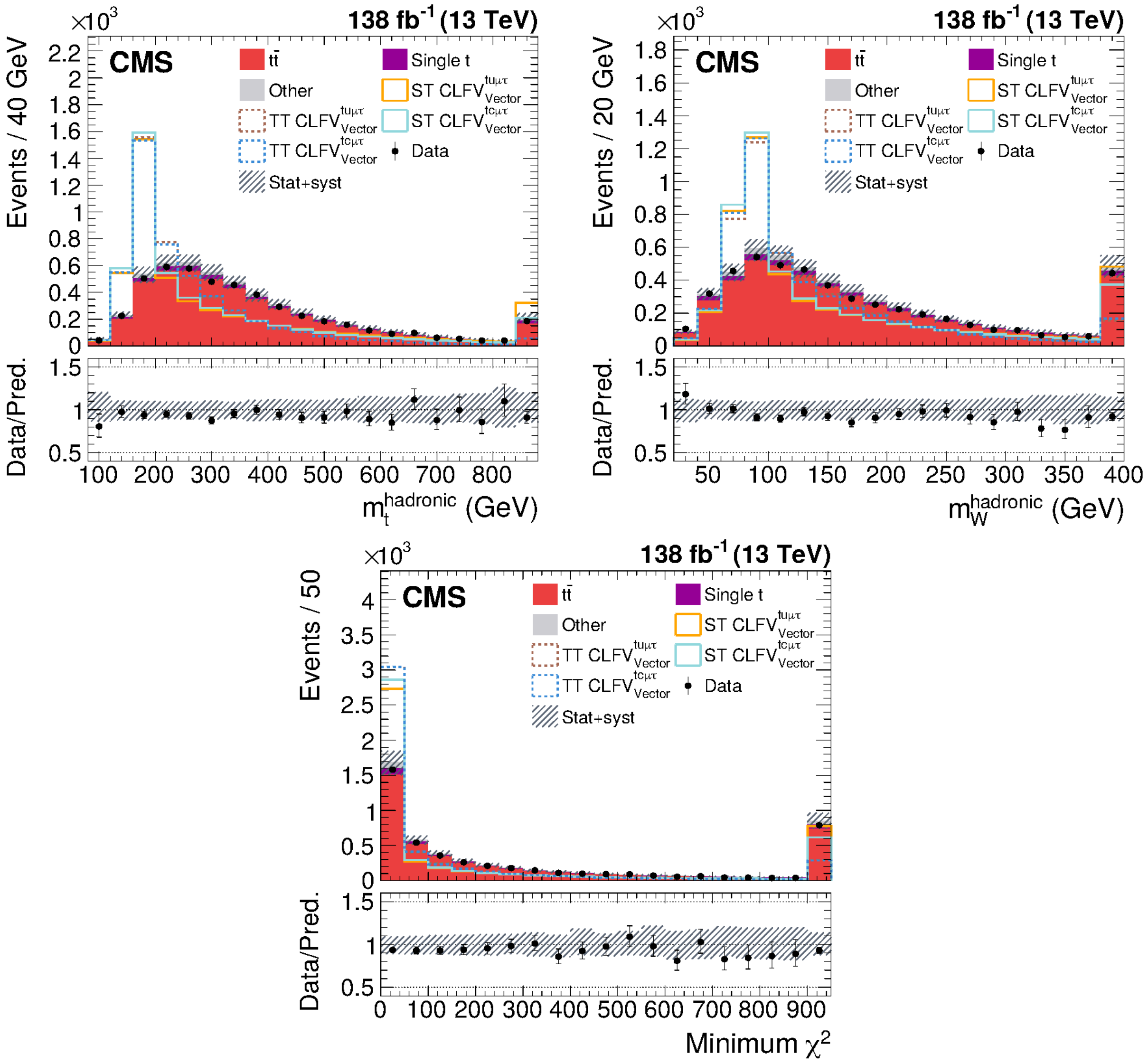

Figure 3: Distributions in the reconstructed top quark mass (upper left), W boson mass (upper right), and minimum χ^2 (lower) from the top quark reconstruction. The solid and dashed lines show the signal distributions, individually for each type of operator and interaction for the vector Lorentz structure as an example. The signals are normalized to the total number of events in data for visibility. The color filled histograms show the stacked background contributions. The data are shown as filled points. The last bin in each histogram contains the overflow. The shaded band displays the total uncertainty in the predicted SM background, consisting of statistical and systematic uncertainties added in quadrature. The panels below the distributions show the ratio of data to the background prediction.

Table 3: Estimated event yields including the background corrections from the ABCD method discussed in Section 5. The numbers shown correspond to observed events before the maximum likelihood fit described in Section 8. Only statistical uncertainties are shown, related to the size of the data sets.

Process	Event yield
ST CLFV tu$\mu\tau$ Scalar	535 ± 1
ST CLFV tu$\mu\tau$ Vector	2327 ± 3
ST CLFV tu$\mu\tau$ Tensor	9909 ± 13
ST CLFV tc$\mu\tau$ Scalar	$32 \pm <1$
ST CLFV tc$\mu\tau$ Vector	$129 \pm <1$
ST CLFV tc$\mu\tau$ Tensor	701 ± 1
TT CLFV tu$\mu\tau$ Scalar	$1.1 \pm <0.1$
TT CLFV tu$\mu\tau$ Vector	$8.2 \pm <0.1$
TT CLFV tu$\mu\tau$ Tensor	$48 \pm <1$
TT CLFV tc$\mu\tau$ Scalar	$1.1 \pm <0.1$
TT CLFV tc$\mu\tau$ Vector	$7.9 \pm <0.1$
TT CLFV tc$\mu\tau$ Tensor	$45 \pm <1$
$t\bar{t}$	4573 ± 13
Single t	306 ± 9
Other	258 ± 5
Total	5136 ± 17
Data	4810

latter have broader distributions because of large contributions from dileptonic $t\bar{t}$ events. Signal events show a noticeable peak at small values in the χ^2 distribution, more pronounced than the background. The data are described by the background simulation within the uncertainties.

6.2 Multivariate analysis using deep neural network

The discrimination between CLFV signals and background processes is performed using machine learning with a multiclass deep neural network (DNN) algorithm.

The input features of the DNN comprise 28 variables, which include kinematic features of individual physics objects and their combinations, and global event features such as p_T^{miss} and variables from the χ^2 reconstruction. The input features together with a short description are given in Table 4. The sensitivity of the DNN classifier is driven by the reconstructed top quark and W boson masses $m_{bjj'}$ and $m_{jj'}$, respectively, as well as the mass of the $\mu\tau_h$ system $m_{\mu\tau_h}$. Following these, the p_T of the muon and τ_h candidates contribute to the classifier performance.

We optimize the DNN design and hyperparameters in terms of its accuracy score. The model is implemented in KERAS [61] with the TENSORFLOW backend [62]. The Adam [63] optimization algorithm is used to minimize the sparse categorical cross-entropy loss function when updating the DNN parameters during the training. The DNN architecture consists of two hidden layers with 50 nodes each, where the weights are initialized with randomly distributed weights following a normal distribution. We use the ReLU [64] activation function and a batch size of 1024 events in the training. The number of training iterations is automatically determined and the training is stopped if there is no improvement in the validation loss after 30 epochs.

The training of the DNN is performed using ST CLFV and TT CLFV signal samples and $t\bar{t}$ background samples. The DNN model is trained to predict the probability p of an event belonging to one of the three classes ST CLFV, TT CLFV, and background. Events after the final selection described in Section 4 are used for the training and the evaluation of the DNN. The three probabilities are combined into a single variable

$$\text{DNN score} = \frac{0.1p(\text{TT CLFV}) + 0.9p(\text{ST CLFV})}{p(\text{background})}, \tag{5}$$

which we found empirically to be an optimal choice for the best expected upper limits on the signal cross sections.

A single DNN classifier is trained for all data-taking periods, combining the different Lorentz structures and the two CLFV interactions $tu\mu\tau$ and $tc\mu\tau$. We balance the number of signal and background events in the training, such that there is no statistical bias from a dominant class. About 150 000 simulated events are passed to the DNN for each of the background and the two signal classes, where 70% are used for the training and 30% for the validation of the DNN.

7 Systematic uncertainties

Systematic uncertainties are considered for experimental sources and the modelling of simulated samples, including uncertainties in the predicted cross sections. The experimental and modelling uncertainties generally change the normalization and the shape of the distributions in the DNN score. The different uncertainty sources are treated as nuisance parameters in a profile likelihood fit in the statistical evaluation of the results. The statistical uncertainties from the limited size of the simulated samples are treated following the Barlow–Beeston-light approach [65].

Table 4: Input features of the DNN. The angular distance ΔR_{ij} between two objects i and j is defined as $\Delta R_{ij} = \sqrt{(\Delta\eta)^2_{ij} + (\Delta\phi)^2_{ij}}$, where $\Delta\eta_{ij}$ and $\Delta\phi_{ij}$ are the differences in pseudorapidity and azimuthal angle, respectively.

Group	Variables	Description
Muon (μ)	$p_{T\mu}$, η_μ	p_T and η of selected muon
Tau (τ_h)	$p_{T\tau_h}$, η_{τ_h}, m_{τ_h}	p_T, η, and mass of selected τ_h
Muon+Tau ($\mu\tau_h$)	$m_{\mu\tau_h}$, $\Delta\eta_{\mu\tau_h}$, $\Delta\phi_{\mu\tau_h}$, $\Delta R_{\mu\tau_h}$	Mass and angular differences of $\mu\tau_h$ system
Jets	p_{T1}, p_{T2}, p_{T3}	p_T of jets ordered in decreasing p_T
	η_1, η_2, η_3	η of jets ordered in decreasing p_T
	m_1, m_2, m_3	Mass of jets ordered in decreasing p_T
	b_1, b_2, b_3	b tagging discriminant of jets ordered in decreasing p_T
Event	p_T^{miss}	Missing transverse momentum
t and W reco.	χ^2, $m_{bjj'}$, $m_{jj'}$	Minimum χ^2 and reconstructed t and W masses
	$\Delta\eta_{jj'}$, $\Delta\phi_{jj'}$, $\Delta R_{jj'}$	Angular differences of jets used in W reco.

7.1 Experimental uncertainties

Integrated luminosity The uncertainties related to the luminosity measurement in each year change the normalization of the signal and background prediction and are 1.2 [66], 2.3 [67], and 2.5% [68] for 2016, 2017, and 2018, respectively. The total uncertainty for all years combined is 1.6%, taking into account correlations in the luminosity measurement between the individual data-taking periods.

Pileup reweighting The uncertainty in the number of pileup interactions is estimated by varying the predicted inelastic cross section of 69.2 mb by ±4.6% [45]. This source is considered to be correlated across all data-taking periods.

Trigger efficiency Data-to-simulation SFs for the trigger efficiency are varied within their uncertainties for each data-taking period and are considered correlated between the periods. In addition, a gradual timing shift of the ECAL was not properly propagated to the first-level trigger inputs and caused an inefficiency by associating the input to the previous bunch crossing in 2016 and 2017, known as "prefiring" [17]. A similar effect is present in the muon system due to the limited time resolution of the subdetectors, mainly affecting the 2016 data, but also present in 2017 and 2018 where the effect is smaller. A corresponding correction is applied, and the uncertainties include a statistical component and a variation of this correction by ±20% [69]. This uncertainty is uncorrelated between data-taking periods.

Muon scale factors We apply corrections because of differences between data and simulation in the track reconstruction, muon identification and isolation efficiencies. The corresponding uncertainties are derived in the determination of these SFs in data samples enriched in $Z \to \mu\mu$ events [20]. In addition to the uncertainties in the SFs, as the reconstruction of high-p_T muons is more challenging and not fully covered by the standard muon identification uncertainties, an uncertainty for muons with p_T larger than 200 GeV is implemented, which increases linearly with increasing p_T [13]. The uncertainties related to the muon identification and isolation are correlated across the data-taking periods.

τ_h identification and energy scale Uncertainties in the identification efficiencies of the τ_h leptons for the discrimination against jets, muons, and electrons consist of several sources related to statistical and systematic components in the scale factor measurement. The uncertainties related to the τ_h candidates discrimination against jets are further divided with respect to the data-taking period, the decay mode of the τ_h, and the p_T range [57]. The uncertainty in the τ_h energy scale is evaluated by shifting the τ_h momentum in simulated events within its uncertainty [56, 57]. The uncertainties in the τ_h identification against jets are partly correlated across the data-taking periods and the τ_h decay modes, depending on the source of uncertainty. Other uncertainties related to the τ_h identification and reconstruction are uncorrelated.

Background estimation for jets misidentified as τ_h The statistical uncertainty arising from the determination of the scaling factors for events with jets misidentified as τ_h candidates is considered. In addition, a closure test is performed using simulated events for individual decay modes of the τ_h candidate and the different data-taking periods. The difference between the number of simulated background events and the number of events predicted by the ABCD method is considered as an uncertainty, and amounts to 2–3%. This uncertainty is uncorrelated for all data-taking periods.

Jet energy scale and resolution The uncertainties in the JES are estimated by shifting the jet momenta in simulated events within their uncertainties for several sources of the JES correction. The JER uncertainty is evaluated by changing the resolution in the simulation by one standard deviation [52]. An inefficiency caused by a non-functional HCAL module in 2018 results in an additional uncertainty [70], which is estimated by scaling down the jet energy in the affected detector region. The JES and JER variations change the p_{T} and the energy of jets and are propagated to $\vec{p}_{\mathrm{T}}^{\,\mathrm{miss}}$. The JES uncertainties are correlated for some sources, while the uncertainties in JER are uncorrelated for all data-taking periods.

b tagging The b tagging uncertainties are derived from SFs applied to correct the tagging efficiency in simulation. The SFs and uncertainties related to the correction of the b tagging discriminant are evaluated separately for light-quark and gluon jets, and for b and c jets [53]. In addition, for each variation of the JES, dedicated scale factors are calculated and applied. The b tagging uncertainty sources include effects from the flavour of jets and statistical uncertainties that arise from the scale factor measurement. The statistical components are uncorrelated between data-taking periods, while the others are fully correlated.

7.2 Modelling uncertainties

The modelling uncertainties are fully correlated through all data-taking periods.

PDF and the strong coupling Uncertainties in the PDF are estimated by reweighting events with the eigenvector variations of the NNPDF 3.1 set [42]. The PDF uncertainty is included for the $\mathrm{t\bar{t}}$ background and signal samples. In addition, an uncertainty from the choice of the strong coupling α_{S} in the PDF set is taken into account [71] for the $\mathrm{t\bar{t}}$ background simulation.

Missing higher orders The uncertainty from missing higher orders in the calculation of matrix elements (ME) for signal and $\mathrm{t\bar{t}}$ background processes is estimated by varying the renormalization (μ_{R}) and factorization (μ_{F}) scales. We consider variations by factors of 2 and 0.5 in μ_{R} at a fixed value of μ_{F}, variations of μ_{F} for a fixed value of μ_{R}, and simultaneous variations of μ_{R} and μ_{F}. The resulting sources of uncertainty are further divided into four different regions in p_{T} of the muon and τ_{h} candidates, to address expected differences arising from additional jets in the TT CLFV signals at high lepton p_{T}.

Parton shower Uncertainties in the initial- and final-state radiation (ISR and FSR) are estimated by varying the scale of α_{S} in the parton shower (PS) by factors of 2 and 0.5 separately for the ISR and FSR. This uncertainty is included for signal and $\mathrm{t\bar{t}}$ background samples.

Cross sections The uncertainties in the predicted cross sections are treated as several different normalization uncertainties. In $\mathrm{t\bar{t}}$ production, scale variations and uncertainties in the PDF amount to a total uncertainty of 4.4% [23]. An uncertainty of 10% is assigned to single top quark production and to all other background processes.

ME-PS matching The damping of high-p_{T} radiation in the matching of the ME and PS simulation is regulated by the parameter h_{damp} in POWHEG [72]. We estimate the uncertainty from the ME-PS matching by shifting $h_{\mathrm{damp}} = 1.58\,^{+0.66}_{-0.59}\,m_{\mathrm{t}}$ within its uncertainties, where $m_{\mathrm{t}} = 172.5\,\mathrm{GeV}$. This uncertainty affects the $\mathrm{t\bar{t}}$ background.

Underlying event The uncertainty related to the CP5 underlying event tune [43] of PYTHIA is evaluated from $\mathrm{t\bar{t}}$ samples generated with modified tune parameters.

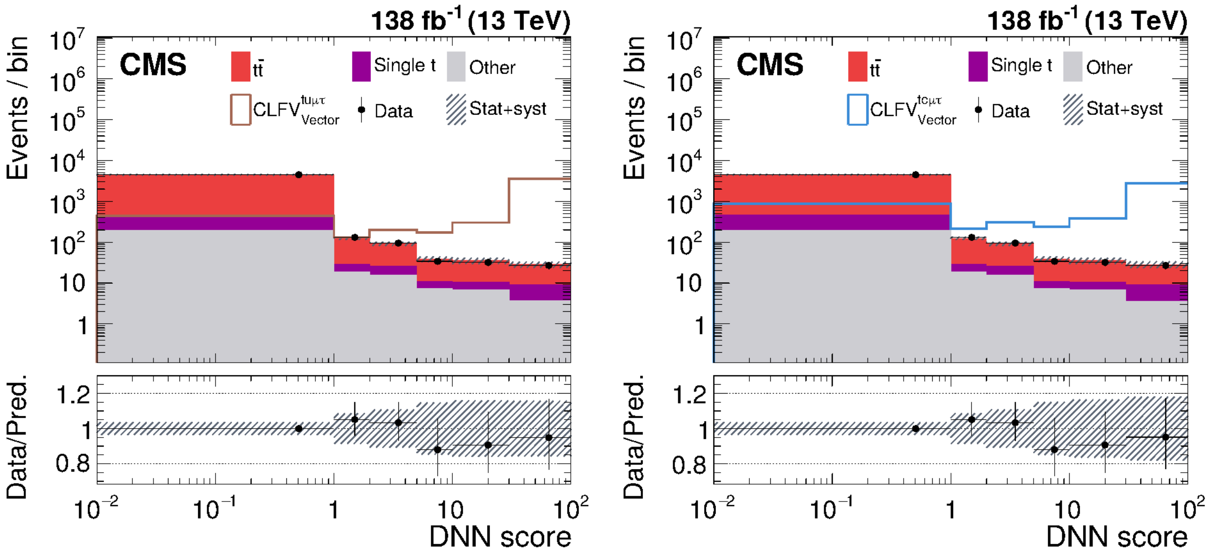

Figure 4: Combined distributions in the DNN score after the profile likelihood fit for all data-taking periods for the vector operators with $tu\mu\tau$ (left) and $tc\mu\tau$ (right) couplings. The signal distributions are normalized to the total number of events observed in the data. The last bin of each histogram contains the overflow. The hatched bands represent the total post-fit uncertainties in the background predictions, including statistical and systematic sources. The panels below the distributions show the ratio of data to the background prediction.

Top quark p_T reweighting The uncertainty arising from the modelling of the top quark p_T spectrum is evaluated by changes in the μ_R and μ_F scales in the NNLO calculation [30] for the determination of the reweighting correction.

8 Results

Distributions in the DNN score are investigated in the search for CLFV interactions. We set upper limits at 95% CL on the coupling modifier $\hat{\mu}$, which translates to limits on the squared Wilson coefficients $(C_a/\Lambda^2)^2$. To set these limits, we use a modified frequentist CL_s method [73, 74], which uses the profile likelihood ratio as the test statistic. The distributions in this test statistic are determined using an asymptotic approximation [75]. A binned maximum likelihood fit is constructed using the measured distribution in the DNN score, the simulated background processes, and the predicted CLFV signals. The systematic uncertainties described in Section 7 are included as nuisance parameters. The statistical analysis is performed using the CMS statistical analysis tool COMBINE [76], which is based on the ROOFIT [77] and ROOSTATS [78] frameworks. Upper limits on the individual coupling modifiers are calculated by performing a simultaneous fit to all data-taking periods.

Distributions in the DNN score are shown for two signal hypotheses in Fig. 4 after the binned maximum likelihood fit for all data-taking periods combined. At the highest value of the DNN score, corresponding to the histogram bin with the highest sensitivity to CLFV interactions, uncertainties of 15–20% in the background predictions are obtained, comparable to the statistical uncertainties in data. We observe no significant deviation from the SM predictions.

We derive one-dimensional upper limits on individual Wilson coefficients. The limits are calculated by taking the square root of the upper limits on the corresponding coupling modifier $\hat{\mu}_a$ for each CLFV interaction operator with $\Lambda = 1\,\text{TeV}$. Upper limits on the branching fractions

Table 5: The 95% CL observed and expected upper limits on CLFV cross sections, Wilson coefficients $C_{tq\mu\tau}$, and branching fractions for different types of interactions and Lorentz structures. The expected upper limits are shown in parentheses after the observed limits. The central probability intervals containing 68% of the expected upper limits are given in square brackets below the upper limits.

Interaction	Type	σ [fb]	$C_{tq\mu\tau}/\Lambda^2$ [TeV^{-2}]	$\mathcal{B}(t \to \mu\tau q)$ [10^{-6}]
$tu\mu\tau$	Scalar	2.039 (2.337) [1.574, 3.594]	0.182 (0.194) [0.160, 0.241]	0.040 (0.046) [0.031, 0.071]
	Vector	2.384 (2.746) [1.857, 4.213]	0.090 (0.096) [0.079, 0.119]	0.078 (0.090) [0.061, 0.138]
	Tensor	2.834 (3.326) [2.257, 5.063]	0.045 (0.049) [0.040, 0.060]	0.118 (0.138) [0.094, 0.211]
$tc\mu\tau$	Scalar	4.269 (5.020) [3.291, 8.142]	0.817 (0.886) [0.717, 1.128]	0.810 (0.953) [0.625, 1.545]
	Vector	7.213 (8.552) [5.663, 13.734]	0.419 (0.457) [0.372, 0.579]	1.710 (2.027) [1.342, 3.255]
	Tensor	7.927 (9.633) [6.427, 15.200]	0.188 (0.207) [0.169, 0.260]	2.052 (2.494) [1.664, 3.936]

$\mathcal{B}(t \to \mu\tau q)$, with $q = u$ or c, are calculated using Eq. (2) from Ref. [24]. Signal processes are considered separately for each Lorentz structure and quark flavour, assuming only one non-vanishing coupling at a time. Limits on the CLFV signal cross sections σ are calculated by multiplying the limit on the coupling modifier with the sum of the ST CLFV and TT CLFV cross sections from Table 2. In Table 5, the observed and expected upper limits on cross sections, Wilson coefficients, and branching fractions for each interaction are listed with the central probability intervals containing 68% of the expected upper limits.

In Fig. 5, we show exclusion contours calculated from the results of Table 5. The contours are obtained with an interpolation by assuming a linear relationship between the limits on $\mathcal{B}(t \to \mu\tau c)$ and $\mathcal{B}(t \to \mu\tau u)$ for each operator. The contours are shown in the plane of branching fractions (left) and Wilson coefficients (right) for the $tu\mu\tau$ and $tc\mu\tau$ couplings for scalar, vector, and tensor operators. In the ST CLFV processes, the cross sections corresponding to the $tu\mu\tau$ coupling are larger than those for the $tc\mu\tau$ coupling, resulting in more stringent constraints on the corresponding Wilson coefficients. The largest impact on the sensitivity of the results originates from the limited sample size in the last bin of the DNN score and the ME scale variations.

9 Summary

A search for charged-lepton flavour violation (CLFV) in the top quark sector has been presented. The search uses data corresponding to an integrated luminosity of 138 fb^{-1} collected by the CMS experiment during 2016–2018 in proton-proton (pp) collisions at $\sqrt{s} = 13$ TeV.

Interactions of a top quark with a muon, a τ lepton, and an up-type quark u or c are considered, where the scale of new physics responsible for CLFV is assumed to be larger than the energy

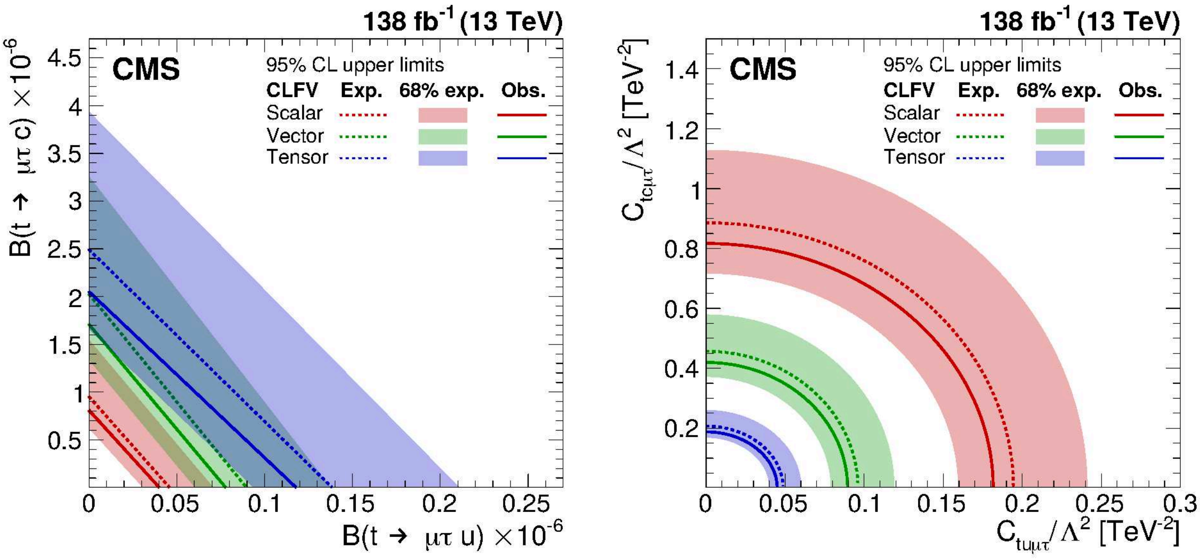

Figure 5: Exclusion contours for the observed and expected 95% CL upper limits and central probability intervals containing 68% of the expected upper limits for the branching fractions (left) and Wilson coefficients (right) corresponding to the tu$\mu\tau$ and tc$\mu\tau$ couplings for scalar, vector and tensor Lorentz structures.

of pp collisions at the LHC. The signal extraction is performed using measured distributions in a multiclass discriminator obtained with a deep neural network. No significant deviation is observed from the standard model background prediction. Upper limits on the signal cross sections are set at 95% confidence level (CL). The limits are interpreted in terms of CLFV branching fractions ($\mathcal{B}$) of the top quark, resulting in $\mathcal{B}(\mathrm{t} \to \mu\tau\mathrm{u}) < (0.040, 0.078, \text{and } 0.118) \times 10^{-6}$, and $\mathcal{B}(\mathrm{t} \to \mu\tau\mathrm{c}) < (0.810, 1.710, \text{and } 2.052) \times 10^{-6}$ at 95% CL for scalar, vector, and tensor-like operators, respectively. This search complements previous CMS results involving eμ CLFV interactions [12, 13] and results in more stringent upper limits on Wilson coefficients in an effective field theory by approximately a factor of two compared to the latest experimental results involving $\mu\tau$ CLFV interactions [11].

Acknowledgments

We congratulate our colleagues in the CERN accelerator departments for the excellent performance of the LHC and thank the technical and administrative staffs at CERN and at other CMS institutes for their contributions to the success of the CMS effort. In addition, we gratefully acknowledge the computing centres and personnel of the Worldwide LHC Computing Grid and other centres for delivering so effectively the computing infrastructure essential to our analyses. Finally, we acknowledge the enduring support for the construction and operation of the LHC, the CMS detector, and the supporting computing infrastructure provided by the following funding agencies: SC (Armenia), BMBWF and FWF (Austria); FNRS and FWO (Belgium); CNPq, CAPES, FAPERJ, FAPERGS, and FAPESP (Brazil); MES and BNSF (Bulgaria); CERN; CAS, MoST, and NSFC (China); MINCIENCIAS (Colombia); MSES and CSF (Croatia); RIF (Cyprus); SENESCYT (Ecuador); ERC PRG, RVTT3 and MoER TK202 (Estonia); Academy of Finland, MEC, and HIP (Finland); CEA and CNRS/IN2P3 (France); SRNSF (Georgia); BMBF, DFG, and HGF (Germany); GSRI (Greece); NKFIH (Hungary); DAE and DST (India); IPM (Iran); SFI (Ireland); INFN (Italy); MSIP and NRF (Republic of Korea); MES (Latvia); LMTLT (Lithuania); MOE and UM (Malaysia); BUAP, CINVESTAV, CONACYT, LNS, SEP, and

UASLP-FAI (Mexico); MOS (Montenegro); MBIE (New Zealand); PAEC (Pakistan); MES and NSC (Poland); FCT (Portugal); MESTD (Serbia); MICIU/AEI and PCTI (Spain); MOSTR (Sri Lanka); Swiss Funding Agencies (Switzerland); MST (Taipei); MHESI and NSTDA (Thailand); TUBITAK and TENMAK (Turkey); NASU (Ukraine); STFC (United Kingdom); DOE and NSF (USA).

Individuals have received support from the Marie-Curie programme and the European Research Council and Horizon 2020 Grant, contract Nos. 675440, 724704, 752730, 758316, 765710, 824093, 101115353, 101002207, and COST Action CA16108 (European Union); the Leventis Foundation; the Alfred P. Sloan Foundation; the Alexander von Humboldt Foundation; the Science Committee, project no. 22rl-037 (Armenia); the Fonds pour la Formation à la Recherche dans l'Industrie et dans l'Agriculture (FRIA-Belgium); the Beijing Municipal Science & Technology Commission, No. Z191100007219010 and Fundamental Research Funds for the Central Universities (China); the Ministry of Education, Youth and Sports (MEYS) of the Czech Republic; the Shota Rustaveli National Science Foundation, grant FR-22-985 (Georgia); the Deutsche Forschungsgemeinschaft (DFG), among others, under Germany's Excellence Strategy – EXC 2121 "Quantum Universe" – 390833306, and under project number 400140256 - GRK2497; the Hellenic Foundation for Research and Innovation (HFRI), Project Number 2288 (Greece); the Hungarian Academy of Sciences, the New National Excellence Program - ÚNKP, the NKFIH research grants K 131991, K 133046, K 138136, K 143460, K 143477, K 146913, K 146914, K 147048, 2020-2.2.1-ED-2021-00181, TKP2021-NKTA-64, and 2021-4.1.2-NEMZ_KI-2024-00036 (Hungary); the Council of Science and Industrial Research, India; ICSC – National Research Centre for High Performance Computing, Big Data and Quantum Computing and FAIR – Future Artificial Intelligence Research, funded by the NextGenerationEU program (Italy); the Latvian Council of Science; the Ministry of Education and Science, project no. 2022/WK/14, and the National Science Center, contracts Opus 2021/41/B/ST2/01369 and 2021/43/B/ST2/01552 (Poland); the Fundação para a Ciência e a Tecnologia, grant CEECIND/01334/2018 (Portugal); the National Priorities Research Program by Qatar National Research Fund; MICIU/AEI/10.13039/501100011033, ERDF/EU, "European Union NextGenerationEU/PRTR", and Programa Severo Ochoa del Principado de Asturias (Spain); the Chulalongkorn Academic into Its 2nd Century Project Advancement Project, and the National Science, Research and Innovation Fund via the Program Management Unit for Human Resources & Institutional Development, Research and Innovation, grant B39G670016 (Thailand); the Kavli Foundation; the Nvidia Corporation; the SuperMicro Corporation; the Welch Foundation, contract C-1845; and the Weston Havens Foundation (USA).

References

[1] R. J. Gaitskell, "Direct detection of dark matter", *Ann. Rev. Nucl. Part. Sci.* **54** (2004) 315, doi:10.1146/annurev.nucl.54.070103.181244.

[2] V. Trimble, "Existence and nature of dark matter in the universe", *Ann. Rev. Astron. Astrophys.* **25** (1987) 425, doi:10.1146/annurev.aa.25.090187.002233.

[3] T. A. Porter, R. P. Johnson, and P. W. Graham, "Dark matter searches with astroparticle data", *Ann. Rev. Astron. Astrophys.* **49** (2011) 155, doi:10.1146/annurev-astro-081710-102528, arXiv:1104.2836.

[4] G. Bertone, D. Hooper, and J. Silk, "Particle dark matter: evidence, candidates and constraints", *Phys. Rept.* **405** (2005) 279, doi:10.1016/j.physrep.2004.08.031, arXiv:hep-ph/0404175.

[5] A. D. Sakharov, "Violation of CP invariance, C asymmetry, and baryon asymmetry of the universe", *Pisma Zh. Eksp. Teor. Fiz.* **5** (1967) 32, doi:10.1070/PU1991v034n05ABEH002497.

[6] R. Davis, Jr., D. S. Harmer, and K. C. Hoffman, "Search for neutrinos from the sun", *Phys. Rev. Lett.* **20** (1968) 1205, doi:10.1103/PhysRevLett.20.1205.

[7] L. Calibbi and G. Signorelli, "Charged lepton flavour violation: An experimental and theoretical introduction", *Riv. Nuovo Cim.* **41** (2018) 71, doi:10.1393/ncr/i2018-10144-0, arXiv:1709.00294.

[8] HFLAV Collaboration, "Averages of b-hadron, c-hadron, and τ-lepton properties as of 2021", *Phys. Rev. D* **107** (2023) 052008, doi:10.1103/PhysRevD.107.052008, arXiv:2206.07501.

[9] T. J. Kim et al., "Correlation between $R_{\mathrm{D}^{(*)}}$ and top quark FCNC decays in leptoquark models", *JHEP* **07** (2019) 025, doi:10.1007/JHEP07(2019)025, arXiv:1812.08484.

[10] LHCb Collaboration, "Measurement of the ratios of branching fractions $\mathcal{R}(\mathrm{D}^*)$ and $\mathcal{R}(\mathrm{D}^0)$", *Phys. Rev. Lett.* **131** (2023) 111802, doi:10.1103/PhysRevLett.131.111802, arXiv:2302.02886.

[11] ATLAS Collaboration, "Search for charged-lepton-flavor violating $\mu\tau$qt interactions in top-quark production and decay in pp collisions at $\sqrt{s} = 13$ TeV with the ATLAS detector at the LHC", *Phys. Rev. D* **110** (2024) 012014, doi:10.1103/PhysRevD.110.012014, arXiv:2403.06742.

[12] CMS Collaboration, "Search for charged-lepton flavor violation in top quark production and decay in pp collisions at $\sqrt{s} = 13$ TeV", *JHEP* **06** (2022) 082, doi:10.1007/JHEP06(2022)082, arXiv:2201.07859.

[13] CMS Collaboration, "Search for charged-lepton flavor violation in the production and decay of top quarks using trilepton final states in proton-proton collisions at $\sqrt{s} = 13$ TeV", *Phys. Rev. D* **111** (2025) 012009, doi:10.1103/PhysRevD.111.012009, arXiv:2312.03199.

[14] J. A. Aguilar-Saavedra et al., "Interpreting top-quark LHC measurements in the standard-model effective field theory", LHC TOP Working Group Public Note CERN-LPCC-2018-01, 2018. arXiv:1802.07237.

[15] B. Grzadkowski, M. Iskrzynski, M. Misiak, and J. Rosiek, "Dimension-six terms in the standard model Lagrangian", *JHEP* **10** (2010) 085, doi:10.1007/JHEP10(2010)085, arXiv:1008.4884.

[16] HEPData record for this analysis, 2025. doi:10.17182/hepdata.153300.

[17] CMS Collaboration, "Performance of the CMS Level-1 trigger in proton-proton collisions at $\sqrt{s} = 13$ TeV", *JINST* **15** (2020) P10017, doi:10.1088/1748-0221/15/10/P10017, arXiv:2006.10165.

[18] CMS Collaboration, "The CMS trigger system", *JINST* **12** (2017) P01020, doi:10.1088/1748-0221/12/01/P01020, arXiv:1609.02366.

[19] CMS Collaboration, "The CMS experiment at the CERN LHC", *JINST* **3** (2008) S08004, doi:10.1088/1748-0221/3/08/S08004.

[20] CMS Collaboration, "Performance of the CMS muon detector and muon reconstruction with proton-proton collisions at $\sqrt{s} = 13\,\text{TeV}$", *JINST* **13** (2018) P06015, doi:10.1088/1748-0221/13/06/P06015, arXiv:1804.04528.

[21] J. Alwall et al., "The automated computation of tree-level and next-to-leading order differential cross sections, and their matching to parton shower simulations", *JHEP* **07** (2014) 079, doi:10.1007/JHEP07(2014)079, arXiv:1405.0301.

[22] A. Dedes et al., "SMEFTFR—Feynman rules generator for the standard model effective field theory", *Comput. Phys. Commun.* **247** (2020) 106931, doi:10.1016/j.cpc.2019.106931, arXiv:1904.03204.

[23] M. Czakon and A. Mitov, "TOP++: a program for the calculation of the top-pair cross-section at hadron colliders", *Comput. Phys. Commun.* **185** (2014) 2930, doi:10.1016/j.cpc.2014.06.021, arXiv:1112.5675.

[24] J. Kile and A. Soni, "Model-independent constraints on lepton-flavor-violating decays of the top quark", *Phys. Rev. D* **78** (2008) 094008, doi:10.1103/PhysRevD.78.094008, arXiv:0807.4199.

[25] J. A. Aguilar-Saavedra, "Effective four-fermion operators in top physics: A roadmap", *Nucl. Phys. B* **843** (2011) 638, doi:10.1016/j.nuclphysb.2010.10.015, arXiv:1008.3562. [Erratum: doi:10.1016/j.nuclphysb.2011.06.003].

[26] I. Brivio, "SMEFTsim 3.0—a practical guide", *JHEP* **04** (2021) 073, doi:10.1007/JHEP04(2021)073, arXiv:2012.11343.

[27] CMS Collaboration, "Measurements of $\mathrm{t\bar{t}}$ differential cross sections in proton-proton collisions at $\sqrt{s} = 13\,\text{TeV}$ using events containing two leptons", *JHEP* **02** (2019) 149, doi:10.1007/JHEP02(2019)149, arXiv:1811.06625.

[28] CMS Collaboration, "Measurement of normalized differential $\mathrm{t\bar{t}}$ cross sections in the dilepton channel from pp collisions at $\sqrt{s} = 13\,\text{TeV}$", *JHEP* **04** (2018) 060, doi:10.1007/JHEP04(2018)060, arXiv:1708.07638.

[29] CMS Collaboration, "Measurement of differential cross sections for top quark pair production using the lepton+jets final state in proton-proton collisions at 13 TeV", *Phys. Rev. D* **95** (2017) 092001, doi:10.1103/PhysRevD.95.092001, arXiv:1610.04191.

[30] M. Czakon et al., "Top-pair production at the LHC through NNLO QCD and NLO EW", *JHEP* **10** (2017) 186, doi:10.1007/JHEP10(2017)186, arXiv:1705.04105.

[31] CMS Collaboration, "Measurement of differential $\mathrm{t\bar{t}}$ production cross sections in the full kinematic range using lepton+jets events from proton-proton collisions at $\sqrt{s} = 13\,\text{TeV}$", *Phys. Rev. D* **104** (2021) 092013, doi:10.1103/PhysRevD.104.092013, arXiv:2108.02803.

[32] P. Nason, "A new method for combining NLO QCD with shower Monte Carlo algorithms", *JHEP* **11** (2004) 040, doi:10.1088/1126-6708/2004/11/040, arXiv:hep-ph/0409146.

[33] S. Frixione, P. Nason, and C. Oleari, “Matching NLO QCD computations with parton shower simulations: the POWHEG method”, *JHEP* **11** (2007) 070, doi:10.1088/1126-6708/2007/11/070, arXiv:0709.2092.

[34] S. Alioli, P. Nason, C. Oleari, and E. Re, “A general framework for implementing NLO calculations in shower Monte Carlo programs: the POWHEG BOX”, *JHEP* **06** (2010) 043, doi:10.1007/JHEP06(2010)043, arXiv:1002.2581.

[35] E. Re, “Single-top Wt-channel production matched with parton showers using the POWHEG method”, *Eur. Phys. J. C* **71** (2011) 1547, doi:10.1140/epjc/s10052-011-1547-z, arXiv:1009.2450.

[36] M. Aliev et al., “HATHOR: Hadronic top and heavy quarks cross section calculator”, *Comput. Phys. Commun.* **182** (2011) 1034, doi:10.1016/j.cpc.2010.12.040, arXiv:1007.1327.

[37] P. Kant et al., “HATHOR for single top-quark production: Updated predictions and uncertainty estimates for single top-quark production in hadronic collisions”, *Comput. Phys. Commun.* **191** (2015) 74, doi:10.1016/j.cpc.2015.02.001, arXiv:1406.4403.

[38] N. Kidonakis, “Two-loop soft anomalous dimensions for single top quark associated production with a W^- or H^-”, *Phys. Rev. D* **82** (2010) 054018, doi:10.1103/PhysRevD.82.054018, arXiv:1005.4451.

[39] N. Kidonakis, “NNLL threshold resummation for top-pair and single-top production”, *Phys. Part. Nucl.* **45** (2014) 714, doi:10.1134/S1063779614040091, arXiv:1210.7813.

[40] J. Alwall et al., “Comparative study of various algorithms for the merging of parton showers and matrix elements in hadronic collisions”, *Eur. Phys. J. C* **53** (2008) 473, doi:10.1140/epjc/s10052-007-0490-5, arXiv:0706.2569.

[41] T. Sjöstrand et al., “An introduction to PYTHIA 8.2”, *Comput. Phys. Commun.* **191** (2015) 159, doi:10.1016/j.cpc.2015.01.024, arXiv:1410.3012.

[42] NNPDF Collaboration, “Parton distributions from high-precision collider data”, *Eur. Phys. J. C* **77** (2017) 663, doi:10.1140/epjc/s10052-017-5199-5, arXiv:1706.00428.

[43] CMS Collaboration, “Extraction and validation of a new set of CMS PYTHIA 8 tunes from underlying-event measurements”, *Eur. Phys. J. C* **80** (2020) 4, doi:10.1140/epjc/s10052-019-7499-4, arXiv:1903.12179.

[44] GEANT4 Collaboration, “GEANT4—a simulation toolkit”, *Nucl. Instrum. Meth. A* **506** (2003) 250, doi:10.1016/S0168-9002(03)01368-8.

[45] CMS Collaboration, “Measurement of the inelastic proton-proton cross section at $\sqrt{s} = 13\,\text{TeV}$”, *JHEP* **07** (2018) 161, doi:10.1007/JHEP07(2018)161, arXiv:1802.02613.

[46] CMS Collaboration, “Particle-flow reconstruction and global event description with the CMS detector”, *JINST* **12** (2017) P10003, doi:10.1088/1748-0221/12/10/P10003, arXiv:1706.04965.

[47] CMS Collaboration, "Technical proposal for the Phase-II upgrade of the Compact Muon Solenoid", CMS Technical Proposal CERN-LHCC-2015-010, CMS-TDR-15-02, 2015. doi:10.17181/CERN.VU8I.D59J.

[48] CMS Collaboration, "Electron and photon reconstruction and identification with the CMS experiment at the CERN LHC", *JINST* **16** (2021) P05014, doi:10.1088/1748-0221/16/05/P05014, arXiv:2012.06888.

[49] M. Cacciari, G. P. Salam, and G. Soyez, "The anti-k_T jet clustering algorithm", *JHEP* **04** (2008) 063, doi:10.1088/1126-6708/2008/04/063, arXiv:0802.1189.

[50] M. Cacciari, G. P. Salam, and G. Soyez, "FASTJET user manual", *Eur. Phys. J. C* **72** (2012) 1896, doi:10.1140/epjc/s10052-012-1896-2, arXiv:1111.6097.

[51] M. Cacciari and G. P. Salam, "Dispelling the N^3 myth for the k_T jet-finder", *Phys. Lett. B* **641** (2006) 57, doi:10.1016/j.physletb.2006.08.037, arXiv:hep-ph/0512210.

[52] CMS Collaboration, "Jet energy scale and resolution in the CMS experiment in pp collisions at 8 TeV", *JINST* **12** (2017) P02014, doi:10.1088/1748-0221/12/02/P02014, arXiv:1607.03663.

[53] CMS Collaboration, "Identification of heavy-flavour jets with the CMS detector in pp collisions at 13 TeV", *JINST* **13** (2018) P05011, doi:10.1088/1748-0221/13/05/P05011, arXiv:1712.07158.

[54] E. Bols et al., "Jet flavour classification using DeepJet", *JINST* **15** (2020) P12012, doi:10.1088/1748-0221/15/12/P12012, arXiv:2008.10519.

[55] CMS Collaboration, "Performance of the DeepJet b tagging algorithm using 41.9 fb^{-1} of data from proton-proton collisions at 13 TeV with Phase 1 CMS detector", CMS Detector Performance Note CMS-DP-2018-058, 2018.

[56] CMS Collaboration, "Performance of reconstruction and identification of τ leptons decaying to hadrons and ν_τ in pp collisions at $\sqrt{s} = 13$ TeV", *JINST* **13** (2018) P10005, doi:10.1088/1748-0221/13/10/P10005, arXiv:1809.02816.

[57] CMS Collaboration, "Identification of hadronic tau lepton decays using a deep neural network", *JINST* **17** (2022) P07023, doi:10.1088/1748-0221/17/07/P07023, arXiv:2201.08458.

[58] CMS Collaboration, "Performance of missing transverse momentum reconstruction in proton-proton collisions at $\sqrt{s} = 13$ TeV using the CMS detector", *JINST* **14** (2019) P07004, doi:10.1088/1748-0221/14/07/P07004, arXiv:1903.06078.

[59] CMS Collaboration, "Measurement of the inclusive W and Z production cross sections in pp collisions at $\sqrt{s} = 7$ TeV with the CMS experiment", *JHEP* **10** (2011) 132, doi:10.1007/JHEP10(2011)132, arXiv:1107.4789.

[60] CDF Collaboration, "Measurement of $\sigma\mathcal{B}(\mathrm{W} \to \mathrm{e}\nu)$ and $\sigma\mathcal{B}(\mathrm{Z}^0 \to \mathrm{e}^+\mathrm{e}^-)$ in $\overline{\mathrm{p}}\mathrm{p}$ collisions at $\sqrt{s} = 1800$ GeV", *Phys. Rev. D* **44** (1991) 29, doi:10.1103/PhysRevD.44.29.

[61] F. Chollet et al., "KERAS", 2015. Software available from https://keras.io.

[62] M. Abadi et al., "TENSORFLOW: Large-scale machine learning on heterogeneous systems", 2015. Software available from http://tensorflow.org. doi:10.5281/zenodo.4724125.

[63] D. P. Kingma and J. Ba, "ADAM: a method for stochastic optimization", in *Proc. 3rd Int. Conf. on Learning Representations (ICLR 2015): San Diego CA, USA, May 7–9, 2015.* 2015. arXiv:1412.6980.

[64] A. F. Agarap, "Deep learning using rectified linear units (ReLU)", 2018. arXiv:1803.08375.

[65] J. S. Conway, "Incorporating nuisance parameters in likelihoods for multisource spectra", in *Proc. 2011 Workshop on Statistical Issues Related to Discovery Claims in Search Experiments and Unfolding (PHYSTAT 2011): Geneva, Switzerland, January 17–20, 2011.* 2011. arXiv:1103.0354. doi:10.5170/CERN-2011-006.115.

[66] CMS Collaboration, "Precision luminosity measurement in proton-proton collisions at $\sqrt{s} = 13$ TeV in 2015 and 2016 at CMS", *Eur. Phys. J. C* **81** (2021) 800, doi:10.1140/epjc/s10052-021-09538-2, arXiv:2104.01927.

[67] CMS Collaboration, "CMS luminosity measurement for the 2017 data-taking period at $\sqrt{s} = 13$ TeV", CMS Physics Analysis Summary CMS-PAS-LUM-17-004, 2018.

[68] CMS Collaboration, "CMS luminosity measurement for the 2018 data-taking period at $\sqrt{s} = 13$ TeV", CMS Physics Analysis Summary CMS-PAS-LUM-18-002, 2019.

[69] CMS Collaboration, "Observation of $\gamma\gamma \to \tau\tau$ in proton-proton collisions and limits on the anomalous electromagnetic moments of the τ lepton", *Rep. Prog. Phys.* **87** (2024) 107801, doi:10.1088/1361-6633/ad6fcb, arXiv:2406.03975.

[70] CMS Collaboration, "Strategies and performance of the CMS silicon tracker alignment during LHC Run 2", *Nucl. Instrum. Meth. A* **1037** (2022) 166795, doi:10.1016/j.nima.2022.166795, arXiv:2111.08757.

[71] J. Butterworth et al., "PDF4LHC recommendations for LHC Run 2", *J. Phys. G* **43** (2016) 023001, doi:10.1088/0954-3899/43/2/023001, arXiv:1510.03865.

[72] CMS Collaboration, "Investigations of the impact of the parton shower tuning in PYTHIA 8 in the modelling of $\mathrm{t\bar{t}}$ at $\sqrt{s} = 8$ and 13 TeV", CMS Physics Analysis Summary CMS-PAS-TOP-16-021, 2016.

[73] T. Junk, "Confidence level computation for combining searches with small statistics", *Nucl. Instrum. Meth. A* **434** (1999) 435, doi:10.1016/S0168-9002(99)00498-2, arXiv:hep-ex/9902006.

[74] A. L. Read, "Presentation of search results: The $\mathrm{CL_s}$ technique", *J. Phys. G* **28** (2002) 2693, doi:10.1088/0954-3899/28/10/313.

[75] G. Cowan, K. Cranmer, E. Gross, and O. Vitells, "Asymptotic formulae for likelihood-based tests of new physics", *Eur. Phys. J. C* **71** (2011) 1554, doi:10.1140/epjc/s10052-011-1554-0, arXiv:1007.1727. [Erratum: doi:10.1140/epjc/s10052-013-2501-z].

[76] CMS Collaboration, "The CMS statistical analysis and combination tool: COMBINE", *Comput. Softw. Big Sci.* **8** (2024) 19, doi:10.1007/s41781-024-00121-4, arXiv:2404.06614.

[77] W. Verkerke and D. Kirkby, "The RooFit toolkit for data modeling", in *Proc. 13th International Conference on Computing in High Energy and Nuclear Physics (CHEP 2003): La Jolla CA, United States, March 24–28, 2003*. 2003. `arXiv:physics/0306116`. [eConf C0303241 (2003) MOLT007].

[78] L. Moneta et al., "The RooStats project", in *Proc. 13th International Workshop on Advanced Computing and Analysis Techniques in Physics Research (ACAT 2010): Jaipur, India, February 22–27, 2010*. 2010. `arXiv:1009.1003`. [PoS (ACAT2010) 057]. `doi:10.22323/1.093.0057`.

A The CMS Collaboration

Yerevan Physics Institute, Yerevan, Armenia
A. Hayrapetyan, A. Tumasyan[1]

Institut für Hochenergiephysik, Vienna, Austria
W. Adam, J.W. Andrejkovic, L. Benato, T. Bergauer, S. Chatterjee, K. Damanakis, M. Dragicevic, P.S. Hussain, M. Jeitler[2], N. Krammer, A. Li, D. Liko, I. Mikulec, J. Schieck[2], R. Schöfbeck[2], D. Schwarz, M. Sonawane, W. Waltenberger, C.-E. Wulz[2]

Universiteit Antwerpen, Antwerpen, Belgium
T. Janssen, T. Van Laer, P. Van Mechelen

Vrije Universiteit Brussel, Brussel, Belgium
N. Breugelmans, J. D'Hondt, S. Dansana, A. De Moor, M. Delcourt, F. Heyen, Y. Hong, S. Lowette, I. Makarenko, D. Müller, S. Tavernier, M. Tytgat[3], G.P. Van Onsem, S. Van Putte, D. Vannerom

Université Libre de Bruxelles, Bruxelles, Belgium
B. Bilin, B. Clerbaux, A.K. Das, I. De Bruyn, G. De Lentdecker, H. Evard, L. Favart, P. Gianneios, A. Khalilzadeh, F.A. Khan, K. Lee, A. Malara, M.A. Shahzad, L. Thomas, M. Vanden Bemden, C. Vander Velde, P. Vanlaer

Ghent University, Ghent, Belgium
M. De Coen, D. Dobur, G. Gokbulut, J. Knolle, L. Lambrecht, D. Marckx, K. Mota Amarilo, K. Skovpen, N. Van Den Bossche, J. van der Linden, L. Wezenbeek

Université Catholique de Louvain, Louvain-la-Neuve, Belgium
S. Bein, A. Benecke, A. Bethani, G. Bruno, C. Caputo, J. De Favereau De Jeneret, C. Delaere, I.S. Donertas, A. Giammanco, A.O. Guzel, Sa. Jain, V. Lemaitre, J. Lidrych, P. Mastrapasqua, T.T. Tran, S. Turkcapar

Centro Brasileiro de Pesquisas Fisicas, Rio de Janeiro, Brazil
G.A. Alves, E. Coelho, G. Correia Silva, C. Hensel, T. Menezes De Oliveira, C. Mora Herrera[4], P. Rebello Teles, M. Soeiro, E.J. Tonelli Manganote[5], A. Vilela Pereira[4]

Universidade do Estado do Rio de Janeiro, Rio de Janeiro, Brazil
W.L. Aldá Júnior, M. Barroso Ferreira Filho, H. Brandao Malbouisson, W. Carvalho, J. Chinellato[6], E.M. Da Costa, G.G. Da Silveira[7], D. De Jesus Damiao, S. Fonseca De Souza, R. Gomes De Souza, T. Laux Kuhn[7], M. Macedo, J. Martins, L. Mundim, H. Nogima, J.P. Pinheiro, A. Santoro, A. Sznajder, M. Thiel

Universidade Estadual Paulista, Universidade Federal do ABC, São Paulo, Brazil
C.A. Bernardes[7], L. Calligaris, T.R. Fernandez Perez Tomei, E.M. Gregores, I. Maietto Silverio, P.G. Mercadante, S.F. Novaes, B. Orzari, Sandra S. Padula

Institute for Nuclear Research and Nuclear Energy, Bulgarian Academy of Sciences, Sofia, Bulgaria
A. Aleksandrov, G. Antchev, R. Hadjiiska, P. Iaydjiev, M. Misheva, M. Shopova, G. Sultanov

University of Sofia, Sofia, Bulgaria

A. Dimitrov, L. Litov, B. Pavlov, P. Petkov, A. Petrov, E. Shumka

Instituto De Alta Investigación, Universidad de Tarapacá, Casilla 7 D, Arica, Chile
S. Keshri, D. Laroze, S. Thakur

Beihang University, Beijing, China
T. Cheng, T. Javaid, L. Yuan

Department of Physics, Tsinghua University, Beijing, China
Z. Hu, Z. Liang, J. Liu

Institute of High Energy Physics, Beijing, China
G.M. Chen[8], H.S. Chen[8], M. Chen[8], F. Iemmi, C.H. Jiang, A. Kapoor[9], H. Liao, Z.-A. Liu[10], R. Sharma[11], J.N. Song[10], J. Tao, C. Wang[8], J. Wang, Z. Wang[8], H. Zhang, J. Zhao

State Key Laboratory of Nuclear Physics and Technology, Peking University, Beijing, China
A. Agapitos, Y. Ban, A. Carvalho Antunes De Oliveira, S. Deng, B. Guo, C. Jiang, A. Levin, C. Li, Q. Li, Y. Mao, S. Qian, S.J. Qian, X. Qin, X. Sun, D. Wang, H. Yang, Y. Zhao, C. Zhou

Guangdong Provincial Key Laboratory of Nuclear Science and Guangdong-Hong Kong Joint Laboratory of Quantum Matter, South China Normal University, Guangzhou, China
S. Yang

Sun Yat-Sen University, Guangzhou, China
Z. You

University of Science and Technology of China, Hefei, China
K. Jaffel, N. Lu

Nanjing Normal University, Nanjing, China
G. Bauer[12], B. Li[13], H. Wang, K. Yi[14], J. Zhang

Institute of Modern Physics and Key Laboratory of Nuclear Physics and Ion-beam Application (MOE) - Fudan University, Shanghai, China
Y. Li

Zhejiang University, Hangzhou, Zhejiang, China
Z. Lin, C. Lu, M. Xiao

Universidad de Los Andes, Bogota, Colombia
C. Avila, D.A. Barbosa Trujillo, A. Cabrera, C. Florez, J. Fraga, J.A. Reyes Vega

Universidad de Antioquia, Medellin, Colombia
J. Jaramillo, C. Rendón, M. Rodriguez, A.A. Ruales Barbosa, J.D. Ruiz Alvarez

University of Split, Faculty of Electrical Engineering, Mechanical Engineering and Naval Architecture, Split, Croatia
D. Giljanovic, N. Godinovic, D. Lelas, A. Sculac

University of Split, Faculty of Science, Split, Croatia
M. Kovac, A. Petkovic, T. Sculac

Institute Rudjer Boskovic, Zagreb, Croatia
P. Bargassa, V. Brigljevic, B.K. Chitroda, D. Ferencek, K. Jakovcic, A. Starodumov[15], T. Susa

University of Cyprus, Nicosia, Cyprus
A. Attikis, K. Christoforou, A. Hadjiagapiou, C. Leonidou, J. Mousa, C. Nicolaou, L. Paizanos, F. Ptochos, P.A. Razis, H. Rykaczewski, H. Saka, A. Stepennov

Charles University, Prague, Czech Republic
M. Finger, M. Finger Jr., A. Kveton

Escuela Politecnica Nacional, Quito, Ecuador
E. Ayala

Universidad San Francisco de Quito, Quito, Ecuador
E. Carrera Jarrin

Academy of Scientific Research and Technology of the Arab Republic of Egypt, Egyptian Network of High Energy Physics, Cairo, Egypt
H. Abdalla[16], Y. Assran[17,18], B. El-mahdy

Center for High Energy Physics (CHEP-FU), Fayoum University, El-Fayoum, Egypt
M. Abdullah Al-Mashad, M.A. Mahmoud

National Institute of Chemical Physics and Biophysics, Tallinn, Estonia
K. Ehataht, M. Kadastik, T. Lange, C. Nielsen, J. Pata, M. Raidal, L. Tani, C. Veelken

Department of Physics, University of Helsinki, Helsinki, Finland
H. Kirschenmann, K. Osterberg, M. Voutilainen

Helsinki Institute of Physics, Helsinki, Finland
S. Bharthuar, N. Bin Norjoharuddeen, E. Brücken, F. Garcia, P. Inkaew, K.T.S. Kallonen, T. Lampén, K. Lassila-Perini, S. Lehti, T. Lindén, M. Myllymäki, M.m. Rantanen, H. Siikonen, J. Tuominiemi

Lappeenranta-Lahti University of Technology, Lappeenranta, Finland
P. Luukka, H. Petrow

IRFU, CEA, Université Paris-Saclay, Gif-sur-Yvette, France
M. Besancon, F. Couderc, M. Dejardin, D. Denegri, J.L. Faure, F. Ferri, S. Ganjour, P. Gras, G. Hamel de Monchenault, M. Kumar, V. Lohezic, J. Malcles, F. Orlandi, L. Portales, A. Rosowsky, M.Ö. Sahin, A. Savoy-Navarro[19], P. Simkina, M. Titov, M. Tornago

Laboratoire Leprince-Ringuet, CNRS/IN2P3, Ecole Polytechnique, Institut Polytechnique de Paris, Palaiseau, France
F. Beaudette, G. Boldrini, P. Busson, A. Cappati, C. Charlot, M. Chiusi, T.D. Cuisset, F. Damas, O. Davignon, A. De Wit, I.T. Ehle, B.A. Fontana Santos Alves, S. Ghosh, A. Gilbert, R. Granier de Cassagnac, A. Hakimi, B. Harikrishnan, L. Kalipoliti, G. Liu, M. Nguyen, C. Ochando, R. Salerno, J.B. Sauvan, Y. Sirois, L. Urda Gómez, E. Vernazza, A. Zabi, A. Zghiche

Université de Strasbourg, CNRS, IPHC UMR 7178, Strasbourg, France
J.-L. Agram[20], J. Andrea, D. Apparu, D. Bloch, J.-M. Brom, E.C. Chabert, C. Collard, S. Falke, U. Goerlach, R. Haeberle, A.-C. Le Bihan, M. Meena, O. Poncet, G. Saha, M.A. Sessini, P. Van Hove, P. Vaucelle

Centre de Calcul de l'Institut National de Physique Nucleaire et de Physique des Particules, CNRS/IN2P3, Villeurbanne, France

A. Di Florio

Institut de Physique des 2 Infinis de Lyon (IP2I), Villeurbanne, France
D. Amram, S. Beauceron, B. Blancon, G. Boudoul, N. Chanon, D. Contardo, P. Depasse, C. Dozen[21], H. El Mamouni, J. Fay, S. Gascon, M. Gouzevitch, C. Greenberg, G. Grenier, B. Ille, E. Jourd'huy, I.B. Laktineh, M. Lethuillier, L. Mirabito, S. Perries, A. Purohit, M. Vander Donckt, P. Verdier, J. Xiao

Georgian Technical University, Tbilisi, Georgia
A. Khvedelidze[15], I. Lomidze, Z. Tsamalaidze[15]

RWTH Aachen University, I. Physikalisches Institut, Aachen, Germany
V. Botta, S. Consuegra Rodríguez, L. Feld, K. Klein, M. Lipinski, D. Meuser, A. Pauls, D. Pérez Adán, N. Röwert, M. Teroerde

RWTH Aachen University, III. Physikalisches Institut A, Aachen, Germany
S. Diekmann, A. Dodonova, N. Eich, D. Eliseev, F. Engelke, J. Erdmann, M. Erdmann, P. Fackeldey, B. Fischer, T. Hebbeker, K. Hoepfner, F. Ivone, A. Jung, M.y. Lee, F. Mausolf, M. Merschmeyer, A. Meyer, S. Mukherjee, D. Noll, F. Nowotny, A. Pozdnyakov, Y. Rath, W. Redjeb, F. Rehm, H. Reithler, V. Sarkisovi, A. Schmidt, C. Seth, A. Sharma, J.L. Spah, A. Stein, F. Torres Da Silva De Araujo[22], S. Wiedenbeck, S. Zaleski

RWTH Aachen University, III. Physikalisches Institut B, Aachen, Germany
C. Dziwok, G. Flügge, T. Kress, A. Nowack, O. Pooth, A. Stahl, T. Ziemons, A. Zotz

Deutsches Elektronen-Synchrotron, Hamburg, Germany
H. Aarup Petersen, M. Aldaya Martin, J. Alimena, S. Amoroso, Y. An, J. Bach, S. Baxter, M. Bayatmakou, H. Becerril Gonzalez, O. Behnke, A. Belvedere, F. Blekman[23], K. Borras[24], A. Campbell, A. Cardini, C. Cheng, F. Colombina, M. De Silva, G. Eckerlin, D. Eckstein, L.I. Estevez Banos, E. Gallo[23], A. Geiser, V. Guglielmi, M. Guthoff, A. Hinzmann, L. Jeppe, B. Kaech, M. Kasemann, C. Kleinwort, R. Kogler, M. Komm, D. Krücker, W. Lange, D. Leyva Pernia, K. Lipka[25], W. Lohmann[26], F. Lorkowski, R. Mankel, I.-A. Melzer-Pellmann, M. Mendizabal Morentin, A.B. Meyer, G. Milella, K. Moral Figueroa, A. Mussgiller, L.P. Nair, J. Niedziela, A. Nürnberg, Y. Otarid, J. Park, E. Ranken, A. Raspereza, D. Rastorguev, J. Rübenach, L. Rygaard, A. Saggio, M. Scham[27,24], S. Schnake[24], P. Schütze, C. Schwanenberger[23], D. Selivanova, K. Sharko, M. Shchedrolosiev, D. Stafford, F. Vazzoler, A. Ventura Barroso, R. Walsh, D. Wang, Q. Wang, K. Wichmann, L. Wiens[24], C. Wissing, Y. Yang, A. Zimermmane Castro Santos

University of Hamburg, Hamburg, Germany
A. Albrecht, S. Albrecht, M. Antonello, S. Bollweg, M. Bonanomi, P. Connor, K. El Morabit, Y. Fischer, E. Garutti, A. Grohsjean, J. Haller, D. Hundhausen, H.R. Jabusch, G. Kasieczka, P. Keicher, R. Klanner, W. Korcari, T. Kramer, C.c. Kuo, V. Kutzner, F. Labe, J. Lange, A. Lobanov, C. Matthies, L. Moureaux, M. Mrowietz, A. Nigamova, Y. Nissan, A. Paasch, K.J. Pena Rodriguez, T. Quadfasel, B. Raciti, M. Rieger, D. Savoiu, J. Schindler, P. Schleper, M. Schröder, J. Schwandt, M. Sommerhalder, H. Stadie, G. Steinbrück, A. Tews, B. Wiederspan, M. Wolf

Karlsruher Institut fuer Technologie, Karlsruhe, Germany
S. Brommer, E. Butz, T. Chwalek, A. Dierlamm, A. Droll, U. Elicabuk, N. Faltermann, M. Giffels, A. Gottmann, F. Hartmann[28], R. Hofsaess, M. Horzela, U. Husemann, J. Kieseler, M. Klute, O. Lavoryk, J.M. Lawhorn, M. Link, A. Lintuluoto, S. Maier, S. Mitra, M. Mormile, Th. Müller, M. Neukum, M. Oh, E. Pfeffer, M. Presilla, G. Quast, K. Rabbertz, B. Regnery, N. Shadskiy, I. Shvetsov, H.J. Simonis, L. Sowa, L. Stockmeier, K. Tauqeer, M. Toms, B. Topko, N. Trevisani, R.F. Von Cube, M. Wassmer, S. Wieland, F. Wittig, R. Wolf, X. Zuo

Institute of Nuclear and Particle Physics (INPP), NCSR Demokritos, Aghia Paraskevi, Greece
G. Anagnostou, G. Daskalakis, A. Kyriakis, A. Papadopoulos[28], A. Stakia

National and Kapodistrian University of Athens, Athens, Greece
G. Melachroinos, Z. Painesis, I. Paraskevas, N. Saoulidou, K. Theofilatos, E. Tziaferi, K. Vellidis, I. Zisopoulos

National Technical University of Athens, Athens, Greece
G. Bakas, T. Chatzistavrou, G. Karapostoli, K. Kousouris, I. Papakrivopoulos, E. Siamarkou, G. Tsipolitis, A. Zacharopoulou

University of Ioánnina, Ioánnina, Greece
I. Bestintzanos, I. Evangelou, C. Foudas, C. Kamtsikis, P. Katsoulis, P. Kokkas, P.G. Kosmoglou Kioseoglou, N. Manthos, I. Papadopoulos, J. Strologas

HUN-REN Wigner Research Centre for Physics, Budapest, Hungary
C. Hajdu, D. Horvath[29,30], K. Márton, A.J. Rádl[31], F. Sikler, V. Veszpremi

MTA-ELTE Lendület CMS Particle and Nuclear Physics Group, Eötvös Loránd University, Budapest, Hungary
M. Csanád, K. Farkas, A. Fehérkuti[32], M.M.A. Gadallah[33], Á. Kadlecsik, P. Major, G. Pásztor, G.I. Veres

Faculty of Informatics, University of Debrecen, Debrecen, Hungary
B. Ujvari, G. Zilizi

HUN-REN ATOMKI - Institute of Nuclear Research, Debrecen, Hungary
G. Bencze, S. Czellar, J. Molnar, Z. Szillasi

Karoly Robert Campus, MATE Institute of Technology, Gyongyos, Hungary
T. Csorgo[32], F. Nemes[32], T. Novak

Panjab University, Chandigarh, India
S. Bansal, S.B. Beri, V. Bhatnagar, G. Chaudhary, S. Chauhan, N. Dhingra[34], A. Kaur, A. Kaur, H. Kaur, M. Kaur, S. Kumar, T. Sheokand, J.B. Singh, A. Singla

University of Delhi, Delhi, India
A. Ahmed, A. Bhardwaj, A. Chhetri, B.C. Choudhary, A. Kumar, A. Kumar, M. Naimuddin, K. Ranjan, M.K. Saini, S. Saumya

Saha Institute of Nuclear Physics, HBNI, Kolkata, India
S. Baradia, S. Barman[35], S. Bhattacharya, S. Das Gupta, S. Dutta, S. Dutta, S. Sarkar

Indian Institute of Technology Madras, Madras, India
M.M. Ameen, P.K. Behera, S.C. Behera, S. Chatterjee, G. Dash, P. Jana,

P. Kalbhor, S. Kamble, J.R. Komaragiri[36], D. Kumar[36], T. Mishra, B. Parida[37], P.R. Pujahari, N.R. Saha, A. Sharma, A.K. Sikdar, R.K. Singh, P. Verma, S. Verma, A. Vijay

Tata Institute of Fundamental Research-A, Mumbai, India
S. Dugad, G.B. Mohanty, M. Shelake, P. Suryadevara

Tata Institute of Fundamental Research-B, Mumbai, India
A. Bala, S. Banerjee, R.M. Chatterjee, M. Guchait, Sh. Jain, A. Jaiswal, S. Kumar, G. Majumder, K. Mazumdar, S. Parolia, A. Thachayath

National Institute of Science Education and Research, An OCC of Homi Bhabha National Institute, Bhubaneswar, Odisha, India
S. Bahinipati[38], C. Kar, D. Maity[39], P. Mal, K. Naskar[39], A. Nayak[39], S. Nayak, K. Pal, P. Sadangi, S.K. Swain, S. Varghese[39], D. Vats[39]

Indian Institute of Science Education and Research (IISER), Pune, India
S. Acharya[40], A. Alpana, S. Dube, B. Gomber[40], P. Hazarika, B. Kansal, A. Laha, B. Sahu[40], S. Sharma, K.Y. Vaish

Isfahan University of Technology, Isfahan, Iran
H. Bakhshiansohi[41], A. Jafari[42], M. Zeinali[43]

Institute for Research in Fundamental Sciences (IPM), Tehran, Iran
S. Bashiri, S. Chenarani[44], S.M. Etesami, Y. Hosseini, M. Khakzad, E. Khazaie, M. Mohammadi Najafabadi, S. Tizchang[45]

University College Dublin, Dublin, Ireland
M. Felcini, M. Grunewald

INFN Sezione di Bari[a], Università di Bari[b], Politecnico di Bari[c], Bari, Italy
M. Abbrescia[a,b], A. Colaleo[a,b], D. Creanza[a,c], B. D'Anzi[a,b], N. De Filippis[a,c], M. De Palma[a,b], W. Elmetenawee[a,b,46], N. Ferrara[a,b], L. Fiore[a], G. Iaselli[a,c], L. Longo[a], M. Louka[a,b], G. Maggi[a,c], M. Maggi[a], I. Margjeka[a], V. Mastrapasqua[a,b], S. My[a,b], S. Nuzzo[a,b], A. Pellecchia[a,b], A. Pompili[a,b], G. Pugliese[a,c], R. Radogna[a,b], D. Ramos[a], A. Ranieri[a], L. Silvestris[a], F.M. Simone[a,c], Ü. Sözbilir[a], A. Stamerra[a,b], D. Troiano[a,b], R. Venditti[a,b], P. Verwilligen[a], A. Zaza[a,b]

INFN Sezione di Bologna[a], Università di Bologna[b], Bologna, Italy
G. Abbiendi[a], C. Battilana[a,b], D. Bonacorsi[a,b], P. Capiluppi[a,b], A. Castro[†a,b], F.R. Cavallo[a], M. Cuffiani[a,b], G.M. Dallavalle[a], T. Diotalevi[a,b], F. Fabbri[a], A. Fanfani[a,b], D. Fasanella[a], P. Giacomelli[a], L. Giommi[a,b], C. Grandi[a], L. Guiducci[a,b], S. Lo Meo[a,47], M. Lorusso[a,b], L. Lunerti[a], S. Marcellini[a], G. Masetti[a], F.L. Navarria[a,b], G. Paggi[a,b], A. Perrotta[a], F. Primavera[a,b], A.M. Rossi[a,b], S. Rossi Tisbeni[a,b], T. Rovelli[a,b], G.P. Siroli[a,b]

INFN Sezione di Catania[a], Università di Catania[b], Catania, Italy
S. Costa[a,b,48], A. Di Mattia[a], A. Lapertosa[a], R. Potenza[a,b], A. Tricomi[a,b,48], C. Tuve[a,b]

INFN Sezione di Firenze[a], Università di Firenze[b], Firenze, Italy
P. Assiouras[a], G. Barbagli[a], G. Bardelli[a,b], B. Camaiani[a,b], A. Cassese[a], R. Ceccarelli[a], V. Ciulli[a,b], C. Civinini[a], R. D'Alessandro[a,b], E. Focardi[a,b], T. Kello[a], G. Latino[a,b], P. Lenzi[a,b], M. Lizzo[a], M. Meschini[a], S. Paoletti[a],

A. Papanastassiou[a,b], G. Sguazzoni[a], L. Viliani[a]

INFN Laboratori Nazionali di Frascati, Frascati, Italy
L. Benussi, S. Bianco, S. Meola[49], D. Piccolo

INFN Sezione di Genova[a], Università di Genova[b], Genova, Italy
M. Alves Gallo Pereira[a], F. Ferro[a], E. Robutti[a], S. Tosi[a,b]

INFN Sezione di Milano-Bicocca[a], Università di Milano-Bicocca[b], Milano, Italy
A. Benaglia[a], F. Brivio[a], F. Cetorelli[a,b], F. De Guio[a,b], M.E. Dinardo[a,b], P. Dini[a], S. Gennai[a], R. Gerosa[a,b], A. Ghezzi[a,b], P. Govoni[a,b], L. Guzzi[a], M.T. Lucchini[a,b], M. Malberti[a], S. Malvezzi[a], A. Massironi[a], D. Menasce[a], L. Moroni[a], M. Paganoni[a,b], S. Palluotto[a,b], D. Pedrini[a], A. Perego[a,b], B.S. Pinolini[a], G. Pizzati[a,b], S. Ragazzi[a,b], T. Tabarelli de Fatis[a,b]

INFN Sezione di Napoli[a], Università di Napoli 'Federico II'[b], Napoli, Italy; Università della Basilicata[c], Potenza, Italy; Scuola Superiore Meridionale (SSM)[d], Napoli, Italy
S. Buontempo[a], A. Cagnotta[a,b], F. Carnevali[a,b], N. Cavallo[a,c], F. Fabozzi[a,c], A.O.M. Iorio[a,b], L. Lista[a,b,50], P. Paolucci[a,28], B. Rossi[a]

INFN Sezione di Padova[a], Università di Padova[b], Padova, Italy; Università di Trento[c], Trento, Italy
R. Ardino[a], P. Azzi[a], N. Bacchetta[a,51], D. Bisello[a,b], P. Bortignon[a], G. Bortolato[a,b], A. Bragagnolo[a,b], A.C.M. Bulla[a], R. Carlin[a,b], P. Checchia[a], T. Dorigo[a,52], S. Fantinel[a], F. Fanzago[a], F. Gasparini[a,b], U. Gasparini[a,b], S. Giorgetti[a], E. Lusiani[a], M. Margoni[a,b], A.T. Meneguzzo[a,b], M. Migliorini[a,b], J. Pazzini[a,b], P. Ronchese[a,b], R. Rossin[a,b], F. Simonetto[a,b], M. Tosi[a,b], A. Triossi[a,b], S. Ventura[a], P. Zotto[a,b], A. Zucchetta[a,b]

INFN Sezione di Pavia[a], Università di Pavia[b], Pavia, Italy
A. Braghieri[a], S. Calzaferri[a], D. Fiorina[a], P. Montagna[a,b], V. Re[a], C. Riccardi[a,b], P. Salvini[a], I. Vai[a,b], P. Vitulo[a,b]

INFN Sezione di Perugia[a], Università di Perugia[b], Perugia, Italy
S. Ajmal[a,b], M.E. Ascioti[a,b], G.M. Bilei[a], C. Carrivale[a,b], D. Ciangottini[a,b], L. Fanò[a,b], M. Magherini[a,b], V. Mariani[a,b], M. Menichelli[a], F. Moscatelli[a,53], A. Rossi[a,b], A. Santocchia[a,b], D. Spiga[a], T. Tedeschi[a,b]

INFN Sezione di Pisa[a], Università di Pisa[b], Scuola Normale Superiore di Pisa[c], Pisa, Italy; Università di Siena[d], Siena, Italy
C. Aimè[a], C.A. Alexe[a,c], P. Asenov[a,b], P. Azzurri[a], G. Bagliesi[a], R. Bhattacharya[a], L. Bianchini[a,b], T. Boccali[a], E. Bossini[a], D. Bruschini[a,c], R. Castaldi[a], M.A. Ciocci[a,b], M. Cipriani[a,b], V. D'Amante[a,d], R. Dell'Orso[a], S. Donato[a,b], A. Giassi[a], F. Ligabue[a,c], A.C. Marini[a,b], D. Matos Figueiredo[a], A. Messineo[a,b], S. Mishra[a], V.K. Muraleedharan Nair Bindhu[a,b,39], M. Musich[a,b], S. Nandan[a], F. Palla[a], A. Rizzi[a,b], G. Rolandi[a,c], S. Roy Chowdhury[a], T. Sarkar[a], A. Scribano[a], P. Spagnolo[a], R. Tenchini[a], G. Tonelli[a,b], N. Turini[a,d], F. Vaselli[a,c], A. Venturi[a], P.G. Verdini[a]

INFN Sezione di Roma[a], Sapienza Università di Roma[b], Roma, Italy
C. Baldenegro Barrera[a,b], P. Barria[a], C. Basile[a,b], F. Cavallari[a], L. Cunqueiro Mendez[a,b], D. Del Re[a,b], E. Di Marco[a,b], M. Diemoz[a], F. Errico[a,b], R. Gargiulo[a,b], E. Longo[a,b], L. Martikainen[a,b], J. Mijuskovic[a,b], G. Organtini[a,b], F. Pandolfi[a], R. Paramatti[a,b], C. Quaranta[a,b], S. Rahatlou[a,b], C. Rovelli[a],

F. Santanastasio[a,b], L. Soffi[a], V. Vladimirov[a,b]

INFN Sezione di Torino[a], Università di Torino[b], Torino, Italy; Università del Piemonte Orientale[c], Novara, Italy
N. Amapane[a,b], R. Arcidiacono[a,c], S. Argiro[a,b], M. Arneodo[a,c], N. Bartosik[a], R. Bellan[a,b], A. Bellora[a,b], C. Biino[a], C. Borca[a,b], N. Cartiglia[a], M. Costa[a,b], R. Covarelli[a,b], N. Demaria[a], L. Finco[a], M. Grippo[a,b], B. Kiani[a,b], F. Legger[a], F. Luongo[a,b], C. Mariotti[a], L. Markovic[a,b], S. Maselli[a], A. Mecca[a,b], L. Menzio[a,b], P. Meridiani[a], E. Migliore[a,b], M. Monteno[a], R. Mulargia[a], M.M. Obertino[a,b], G. Ortona[a], L. Pacher[a,b], N. Pastrone[a], M. Pelliccioni[a], M. Ruspa[a,c], F. Siviero[a,b], V. Sola[a,b], A. Solano[a,b], A. Staiano[a], C. Tarricone[a,b], D. Trocino[a], G. Umoret[a,b], R. White[a,b]

INFN Sezione di Trieste[a], Università di Trieste[b], Trieste, Italy
J. Babbar[a,b], S. Belforte[a], V. Candelise[a,b], M. Casarsa[a], F. Cossutti[a], K. De Leo[a], G. Della Ricca[a,b]

Kyungpook National University, Daegu, Korea
S. Dogra, J. Hong, B. Kim, J. Kim, D. Lee, H. Lee, S.W. Lee, C.S. Moon, Y.D. Oh, M.S. Ryu, S. Sekmen, B. Tae, Y.C. Yang

Department of Mathematics and Physics - GWNU, Gangneung, Korea
M.S. Kim

Chonnam National University, Institute for Universe and Elementary Particles, Kwangju, Korea
G. Bak, P. Gwak, H. Kim, D.H. Moon

Hanyang University, Seoul, Korea
E. Asilar, J. Choi[54], D. Kim, T.J. Kim, J.A. Merlin, Y. Ryou

Korea University, Seoul, Korea
S. Choi, S. Han, B. Hong, K. Lee, K.S. Lee, S. Lee, J. Yoo

Kyung Hee University, Department of Physics, Seoul, Korea
J. Goh, S. Yang

Sejong University, Seoul, Korea
H. S. Kim, Y. Kim, S. Lee

Seoul National University, Seoul, Korea
J. Almond, J.H. Bhyun, J. Choi, J. Choi, W. Jun, J. Kim, Y.W. Kim, S. Ko, H. Kwon, H. Lee, J. Lee, J. Lee, B.H. Oh, S.B. Oh, H. Seo, U.K. Yang, I. Yoon

University of Seoul, Seoul, Korea
W. Jang, D.Y. Kang, Y. Kang, S. Kim, B. Ko, J.S.H. Lee, Y. Lee, I.C. Park, Y. Roh, I.J. Watson

Yonsei University, Department of Physics, Seoul, Korea
S. Ha, K. Hwang, H.D. Yoo

Sungkyunkwan University, Suwon, Korea
M. Choi, M.R. Kim, H. Lee, Y. Lee, I. Yu

College of Engineering and Technology, American University of the Middle East (AUM), Dasman, Kuwait

T. Beyrouthy, Y. Gharbia

Kuwait University - College of Science - Department of Physics, Safat, Kuwait
F. Alazemi

Riga Technical University, Riga, Latvia
K. Dreimanis, A. Gaile, C. Munoz Diaz, D. Osite, G. Pikurs, A. Potrebko, M. Seidel, D. Sidiropoulos Kontos

University of Latvia (LU), Riga, Latvia
N.R. Strautnieks

Vilnius University, Vilnius, Lithuania
M. Ambrozas, A. Juodagalvis, A. Rinkevicius, G. Tamulaitis

National Centre for Particle Physics, Universiti Malaya, Kuala Lumpur, Malaysia
I. Yusuff[55], Z. Zolkapli

Universidad de Sonora (UNISON), Hermosillo, Mexico
J.F. Benitez, A. Castaneda Hernandez, H.A. Encinas Acosta, L.G. Gallegos Maríñez, M. León Coello, J.A. Murillo Quijada, A. Sehrawat, L. Valencia Palomo

Centro de Investigacion y de Estudios Avanzados del IPN, Mexico City, Mexico
G. Ayala, H. Castilla-Valdez, H. Crotte Ledesma, E. De La Cruz-Burelo, I. Heredia-De La Cruz[56], R. Lopez-Fernandez, J. Mejia Guisao, C.A. Mondragon Herrera, A. Sánchez Hernández

Universidad Iberoamericana, Mexico City, Mexico
C. Oropeza Barrera, D.L. Ramirez Guadarrama, M. Ramírez García

Benemerita Universidad Autonoma de Puebla, Puebla, Mexico
I. Bautista, F.E. Neri Huerta, I. Pedraza, H.A. Salazar Ibarguen, C. Uribe Estrada

University of Montenegro, Podgorica, Montenegro
I. Bubanja, N. Raicevic

University of Canterbury, Christchurch, New Zealand
P.H. Butler

National Centre for Physics, Quaid-I-Azam University, Islamabad, Pakistan
A. Ahmad, M.I. Asghar, A. Awais, M.I.M. Awan, H.R. Hoorani, W.A. Khan

AGH University of Krakow, Krakow, Poland
V. Avati, L. Grzanka, M. Malawski

National Centre for Nuclear Research, Swierk, Poland
H. Bialkowska, M. Bluj, M. Górski, M. Kazana, M. Szleper, P. Zalewski

Institute of Experimental Physics, Faculty of Physics, University of Warsaw, Warsaw, Poland
K. Bunkowski, K. Doroba, A. Kalinowski, M. Konecki, J. Krolikowski, A. Muhammad

Warsaw University of Technology, Warsaw, Poland
P. Fokow, K. Pozniak, W. Zabolotny

Laboratório de Instrumentação e Física Experimental de Partículas, Lisboa, Portugal
M. Araujo, D. Bastos, C. Beirão Da Cruz E Silva, A. Boletti, M. Bozzo, T. Camporesi, G. Da Molin, P. Faccioli, M. Gallinaro, J. Hollar, N. Leonardo,

G.B. Marozzo, A. Petrilli, M. Pisano, J. Seixas, J. Varela, J.W. Wulff

Faculty of Physics, University of Belgrade, Belgrade, Serbia
P. Adzic, P. Milenovic

VINCA Institute of Nuclear Sciences, University of Belgrade, Belgrade, Serbia
D. Devetak, M. Dordevic, J. Milosevic, L. Nadderd, V. Rekovic

Centro de Investigaciones Energéticas Medioambientales y Tecnológicas (CIEMAT), Madrid, Spain
J. Alcaraz Maestre, Cristina F. Bedoya, J.A. Brochero Cifuentes, Oliver M. Carretero, M. Cepeda, M. Cerrada, N. Colino, B. De La Cruz, A. Delgado Peris, A. Escalante Del Valle, D. Fernández Del Val, J.P. Fernández Ramos, J. Flix, M.C. Fouz, O. Gonzalez Lopez, S. Goy Lopez, J.M. Hernandez, M.I. Josa, J. Llorente Merino, C. Martin Perez, E. Martin Viscasillas, D. Moran, C. M. Morcillo Perez, Á. Navarro Tobar, C. Perez Dengra, A. Pérez-Calero Yzquierdo, J. Puerta Pelayo, I. Redondo, S. Sánchez Navas, J. Sastre, J. Vazquez Escobar

Universidad Autónoma de Madrid, Madrid, Spain
J.F. de Trocóniz

Universidad de Oviedo, Instituto Universitario de Ciencias y Tecnologías Espaciales de Asturias (ICTEA), Oviedo, Spain
B. Alvarez Gonzalez, J. Cuevas, J. Fernandez Menendez, S. Folgueras, I. Gonzalez Caballero, P. Leguina, E. Palencia Cortezon, J. Prado Pico, C. Ramón Álvarez, V. Rodríguez Bouza, A. Soto Rodríguez, A. Trapote, C. Vico Villalba, P. Vischia

Instituto de Física de Cantabria (IFCA), CSIC-Universidad de Cantabria, Santander, Spain
S. Bhowmik, S. Blanco Fernández, I.J. Cabrillo, A. Calderon, J. Duarte Campderros, M. Fernandez, G. Gomez, C. Lasaosa García, R. Lopez Ruiz, C. Martinez Rivero, P. Martinez Ruiz del Arbol, F. Matorras, P. Matorras Cuevas, E. Navarrete Ramos, J. Piedra Gomez, L. Scodellaro, I. Vila, J.M. Vizan Garcia

University of Colombo, Colombo, Sri Lanka
B. Kailasapathy[57], D.D.C. Wickramarathna

University of Ruhuna, Department of Physics, Matara, Sri Lanka
W.G.D. Dharmaratna[58], K. Liyanage, N. Perera

CERN, European Organization for Nuclear Research, Geneva, Switzerland
D. Abbaneo, C. Amendola, E. Auffray, G. Auzinger, J. Baechler, D. Barney, A. Bermúdez Martínez, M. Bianco, A.A. Bin Anuar, A. Bocci, L. Borgonovi, C. Botta, E. Brondolin, C.E. Brown, C. Caillol, G. Cerminara, N. Chernyavskaya, D. d'Enterria, A. Dabrowski, A. David, A. De Roeck, M.M. Defranchis, M. Deile, M. Dobson, G. Franzoni, W. Funk, S. Giani, D. Gigi, K. Gill, F. Glege, J. Hegeman, J.K. Heikkilä, B. Huber, V. Innocente, T. James, P. Janot, O. Kaluzinska, O. Karacheban[26], G. Karathanasis, S. Laurila, P. Lecoq, E. Leutgeb, C. Lourenço, L. Malgeri, M. Mannelli, M. Matthewman, A. Mehta, F. Meijers, S. Mersi, E. Meschi, V. Milosevic, F. Monti, F. Moortgat, M. Mulders, I. Neutelings, S. Orfanelli, F. Pantaleo, G. Petrucciani, A. Pfeiffer, M. Pierini, H. Qu, D. Rabady, B. Ribeiro Lopes, F. Riti, M. Rovere, H. Sakulin, R. Salvatico, S. Sanchez Cruz, S. Scarfi, C. Schwick, M. Selvaggi, A. Sharma, K. Shchelina, P. Silva, P. Sphicas[59], A.G. Stahl Leiton, A. Steen, S. Summers, D. Treille, P. Tropea, D. Walter, J. Wanczyk[60], J. Wang, S. Wuchterl, P. Zehetner, P. Zejdl, W.D. Zeuner

PSI Center for Neutron and Muon Sciences, Villigen, Switzerland
T. Bevilacqua[61], L. Caminada[61], A. Ebrahimi, W. Erdmann, R. Horisberger, Q. Ingram, H.C. Kaestli, D. Kotlinski, C. Lange, M. Missiroli[61], L. Noehte[61], T. Rohe, A. Samalan

ETH Zurich - Institute for Particle Physics and Astrophysics (IPA), Zurich, Switzerland
T.K. Aarrestad, M. Backhaus, G. Bonomelli, A. Calandri, C. Cazzaniga, K. Datta, P. De Bryas Dexmiers D'archiac[60], A. De Cosa, G. Dissertori, M. Dittmar, M. Donegà, F. Eble, M. Galli, K. Gedia, F. Glessgen, C. Grab, N. Härringer, T.G. Harte, D. Hits, W. Lustermann, A.-M. Lyon, R.A. Manzoni, M. Marchegiani, L. Marchese, A. Mascellani[60], F. Nessi-Tedaldi, F. Pauss, V. Perovic, S. Pigazzini, B. Ristic, R. Seidita, J. Steggemann[60], A. Tarabini, D. Valsecchi, R. Wallny

Universität Zürich, Zurich, Switzerland
C. Amsler[62], P. Bärtschi, M.F. Canelli, K. Cormier, M. Huwiler, W. Jin, A. Jofrehei, B. Kilminster, S. Leontsinis, S.P. Liechti, A. Macchiolo, P. Meiring, F. Meng, J. Motta, A. Reimers, P. Robmann, M. Senger, E. Shokr, F. Stäger, R. Tramontano

National Central University, Chung-Li, Taiwan
C. Adloff[63], D. Bhowmik, C.M. Kuo, W. Lin, P.K. Rout, P.C. Tiwari[36]

National Taiwan University (NTU), Taipei, Taiwan
L. Ceard, K.F. Chen, Z.g. Chen, A. De Iorio, W.-S. Hou, T.h. Hsu, Y.w. Kao, S. Karmakar, G. Kole, Y.y. Li, R.-S. Lu, E. Paganis, X.f. Su, J. Thomas-Wilsker, L.s. Tsai, D. Tsionou, H.y. Wu, E. Yazgan

High Energy Physics Research Unit, Department of Physics, Faculty of Science, Chulalongkorn University, Bangkok, Thailand
C. Asawatangtrakuldee, N. Srimanobhas, V. Wachirapusitanand

Tunis El Manar University, Tunis, Tunisia
Y. Maghrbi

Çukurova University, Physics Department, Science and Art Faculty, Adana, Turkey
D. Agyel, F. Boran, F. Dolek, I. Dumanoglu[64], E. Eskut, Y. Guler[65], E. Gurpinar Guler[65], C. Isik, O. Kara, A. Kayis Topaksu, Y. Komurcu, G. Onengut, K. Ozdemir[66], A. Polatoz, B. Tali[67], U.G. Tok, E. Uslan, I.S. Zorbakir

Middle East Technical University, Physics Department, Ankara, Turkey
G. Sokmen, M. Yalvac[68]

Bogazici University, Istanbul, Turkey
B. Akgun, I.O. Atakisi, E. Gülmez, M. Kaya[69], O. Kaya[70], S. Tekten[71]

Istanbul Technical University, Istanbul, Turkey
A. Cakir, K. Cankocak[64,72], G.G. Dincer[64], S. Sen[73]

Istanbul University, Istanbul, Turkey
O. Aydilek[74], B. Hacisahinoglu, I. Hos[75], B. Kaynak, S. Ozkorucuklu, O. Potok, H. Sert, C. Simsek, C. Zorbilmez

Yildiz Technical University, Istanbul, Turkey
S. Cerci, B. Isildak[76], D. Sunar Cerci, T. Yetkin

Institute for Scintillation Materials of National Academy of Science of Ukraine, Kharkiv,

Ukraine
A. Boyaryntsev, B. Grynyov

National Science Centre, Kharkiv Institute of Physics and Technology, Kharkiv, Ukraine
L. Levchuk

University of Bristol, Bristol, United Kingdom
D. Anthony, J.J. Brooke, A. Bundock, F. Bury, E. Clement, D. Cussans, H. Flacher, M. Glowacki, J. Goldstein, H.F. Heath, M.-L. Holmberg, L. Kreczko, S. Paramesvaran, L. Robertshaw, V.J. Smith, K. Walkingshaw Pass

Rutherford Appleton Laboratory, Didcot, United Kingdom
A.H. Ball, K.W. Bell, A. Belyaev[77], C. Brew, R.M. Brown, D.J.A. Cockerill, C. Cooke, A. Elliot, K.V. Ellis, K. Harder, S. Harper, J. Linacre, K. Manolopoulos, D.M. Newbold, E. Olaiya, D. Petyt, T. Reis, A.R. Sahasransu, G. Salvi, T. Schuh, C.H. Shepherd-Themistocleous, I.R. Tomalin, K.C. Whalen, T. Williams

Imperial College, London, United Kingdom
I. Andreou, R. Bainbridge, P. Bloch, O. Buchmuller, C.A. Carrillo Montoya, G.S. Chahal[78], D. Colling, J.S. Dancu, I. Das, P. Dauncey, G. Davies, M. Della Negra, S. Fayer, G. Fedi, G. Hall, A. Howard, G. Iles, C.R. Knight, P. Krueper, J. Langford, K.H. Law, J. León Holgado, L. Lyons, A.-M. Magnan, B. Maier, S. Mallios, M. Mieskolainen, J. Nash[79], M. Pesaresi, P.B. Pradeep, B.C. Radburn-Smith, A. Richards, A. Rose, K. Savva, C. Seez, R. Shukla, A. Tapper, K. Uchida, G.P. Uttley, T. Virdee[28], M. Vojinovic, N. Wardle, D. Winterbottom

Brunel University, Uxbridge, United Kingdom
J.E. Cole, A. Khan, P. Kyberd, I.D. Reid

Baylor University, Waco, Texas, USA
S. Abdullin, A. Brinkerhoff, E. Collins, M.R. Darwish, J. Dittmann, K. Hatakeyama, V. Hegde, J. Hiltbrand, B. McMaster, J. Samudio, S. Sawant, C. Sutantawibul, J. Wilson

Catholic University of America, Washington, DC, USA
R. Bartek, A. Dominguez, A.E. Simsek, S.S. Yu

The University of Alabama, Tuscaloosa, Alabama, USA
B. Bam, A. Buchot Perraguin, R. Chudasama, S.I. Cooper, C. Crovella, S.V. Gleyzer, E. Pearson, C.U. Perez, P. Rumerio[80], E. Usai, R. Yi

Boston University, Boston, Massachusetts, USA
A. Akpinar, C. Cosby, G. De Castro, Z. Demiragli, C. Erice, C. Fangmeier, C. Fernandez Madrazo, E. Fontanesi, D. Gastler, F. Golf, S. Jeon, J. O'cain, I. Reed, J. Rohlf, K. Salyer, D. Sperka, D. Spitzbart, I. Suarez, A. Tsatsos, A.G. Zecchinelli

Brown University, Providence, Rhode Island, USA
G. Barone, G. Benelli, D. Cutts, L. Gouskos, M. Hadley, U. Heintz, K.W. Ho, J.M. Hogan[81], T. Kwon, G. Landsberg, K.T. Lau, J. Luo, S. Mondal, T. Russell, S. Sagir[82], X. Shen, F. Simpson, M. Stamenkovic, N. Venkatasubramanian

University of California, Davis, Davis, California, USA
S. Abbott, B. Barton, C. Brainerd, R. Breedon, H. Cai,

M. Calderon De La Barca Sanchez, M. Chertok, M. Citron, J. Conway, P.T. Cox, R. Erbacher, F. Jensen, O. Kukral, G. Mocellin, M. Mulhearn, S. Ostrom, W. Wei, S. Yoo, F. Zhang

University of California, Los Angeles, California, USA
K. Adamidis, M. Bachtis, D. Campos, R. Cousins, A. Datta, G. Flores Avila, J. Hauser, M. Ignatenko, M.A. Iqbal, T. Lam, Y.f. Lo, E. Manca, A. Nunez Del Prado, D. Saltzberg, V. Valuev

University of California, Riverside, Riverside, California, USA
R. Clare, J.W. Gary, G. Hanson

University of California, San Diego, La Jolla, California, USA
A. Aportela, A. Arora, J.G. Branson, S. Cittolin, S. Cooperstein, D. Diaz, J. Duarte, L. Giannini, Y. Gu, J. Guiang, R. Kansal, V. Krutelyov, R. Lee, J. Letts, M. Masciovecchio, F. Mokhtar, S. Mukherjee, M. Pieri, D. Primosch, M. Quinnan, V. Sharma, M. Tadel, E. Vourliotis, F. Würthwein, Y. Xiang, A. Yagil

University of California, Santa Barbara - Department of Physics, Santa Barbara, California, USA
A. Barzdukas, L. Brennan, C. Campagnari, K. Downham, C. Grieco, M.M. Hussain, J. Incandela, J. Kim, A.J. Li, P. Masterson, H. Mei, J. Richman, S.N. Santpur, U. Sarica, R. Schmitz, F. Setti, J. Sheplock, D. Stuart, T.Á. Vámi, X. Yan, D. Zhang

California Institute of Technology, Pasadena, California, USA
S. Bhattacharya, A. Bornheim, O. Cerri, A. Latorre, J. Mao, H.B. Newman, G. Reales Gutiérrez, M. Spiropulu, J.R. Vlimant, C. Wang, S. Xie, R.Y. Zhu

Carnegie Mellon University, Pittsburgh, Pennsylvania, USA
J. Alison, S. An, P. Bryant, M. Cremonesi, V. Dutta, T. Ferguson, T.A. Gómez Espinosa, A. Harilal, A. Kallil Tharayil, C. Liu, T. Mudholkar, S. Murthy, P. Palit, K. Park, M. Paulini, A. Roberts, A. Sanchez, W. Terrill

University of Colorado Boulder, Boulder, Colorado, USA
J.P. Cumalat, W.T. Ford, A. Hart, A. Hassani, N. Manganelli, J. Pearkes, C. Savard, N. Schonbeck, K. Stenson, K.A. Ulmer, S.R. Wagner, N. Zipper, D. Zuolo

Cornell University, Ithaca, New York, USA
J. Alexander, S. Bright-Thonney, X. Chen, D.J. Cranshaw, J. Dickinson, J. Fan, X. Fan, S. Hogan, P. Kotamnives, J. Monroy, M. Oshiro, J.R. Patterson, M. Reid, A. Ryd, J. Thom, P. Wittich, R. Zou

Fermi National Accelerator Laboratory, Batavia, Illinois, USA
M. Albrow, M. Alyari, O. Amram, G. Apollinari, A. Apresyan, L.A.T. Bauerdick, D. Berry, J. Berryhill, P.C. Bhat, K. Burkett, J.N. Butler, A. Canepa, G.B. Cerati, H.W.K. Cheung, F. Chlebana, G. Cummings, I. Dutta, V.D. Elvira, Y. Feng, J. Freeman, A. Gandrakota, Z. Gecse, L. Gray, D. Green, A. Grummer, S. Grünendahl, D. Guerrero, O. Gutsche, R.M. Harris, T.C. Herwig, J. Hirschauer, B. Jayatilaka, S. Jindariani, M. Johnson, U. Joshi, T. Klijnsma, B. Klima, K.H.M. Kwok, S. Lammel, C. Lee, D. Lincoln, R. Lipton, T. Liu, C. Madrid, K. Maeshima, D. Mason, P. McBride, P. Merkel, S. Mrenna,

S. Nahn, J. Ngadiuba, D. Noonan, S. Norberg, V. Papadimitriou, N. Pastika, K. Pedro, C. Pena[83], F. Ravera, A. Reinsvold Hall[84], L. Ristori, M. Safdari, E. Sexton-Kennedy, N. Smith, A. Soha, L. Spiegel, S. Stoynev, J. Strait, L. Taylor, S. Tkaczyk, N.V. Tran, L. Uplegger, E.W. Vaandering, I. Zoi

University of Florida, Gainesville, Florida, USA
C. Aruta, P. Avery, D. Bourilkov, P. Chang, V. Cherepanov, R.D. Field, C. Huh, E. Koenig, M. Kolosova, J. Konigsberg, A. Korytov, K. Matchev, N. Menendez, G. Mitselmakher, K. Mohrman, A. Muthirakalayil Madhu, N. Rawal, S. Rosenzweig, Y. Takahashi, J. Wang

Florida State University, Tallahassee, Florida, USA
T. Adams, A. Al Kadhim, A. Askew, S. Bower, R. Hashmi, R.S. Kim, S. Kim, T. Kolberg, G. Martinez, H. Prosper, P.R. Prova, M. Wulansatiti, R. Yohay, J. Zhang

Florida Institute of Technology, Melbourne, Florida, USA
B. Alsufyani, S. Butalla, S. Das, T. Elkafrawy[85], M. Hohlmann, E. Yanes

University of Illinois Chicago, Chicago, Illinois, USA
M.R. Adams, A. Baty, C. Bennett, R. Cavanaugh, R. Escobar Franco, O. Evdokimov, C.E. Gerber, M. Hawksworth, A. Hingrajiya, D.J. Hofman, J.h. Lee, D. S. Lemos, A.H. Merrit, C. Mills, S. Nanda, G. Oh, B. Ozek, D. Pilipovic, R. Pradhan, E. Prifti, T. Roy, S. Rudrabhatla, N. Singh, M.B. Tonjes, N. Varelas, M.A. Wadud, Z. Ye, J. Yoo

The University of Iowa, Iowa City, Iowa, USA
M. Alhusseini, D. Blend, K. Dilsiz[86], L. Emediato, G. Karaman, O.K. Köseyan, J.-P. Merlo, A. Mestvirishvili[87], O. Neogi, H. Ogul[88], Y. Onel, A. Penzo, C. Snyder, E. Tiras[89]

Johns Hopkins University, Baltimore, Maryland, USA
B. Blumenfeld, L. Corcodilos, J. Davis, A.V. Gritsan, L. Kang, S. Kyriacou, P. Maksimovic, M. Roguljic, J. Roskes, S. Sekhar, M. Swartz

The University of Kansas, Lawrence, Kansas, USA
A. Abreu, L.F. Alcerro Alcerro, J. Anguiano, S. Arteaga Escatel, P. Baringer, A. Bean, Z. Flowers, D. Grove, J. King, G. Krintiras, M. Lazarovits, C. Le Mahieu, J. Marquez, M. Murray, M. Nickel, M. Pitt, S. Popescu[90], C. Rogan, C. Royon, S. Sanders, C. Smith, G. Wilson

Kansas State University, Manhattan, Kansas, USA
B. Allmond, R. Gujju Gurunadha, A. Ivanov, K. Kaadze, Y. Maravin, J. Natoli, D. Roy, G. Sorrentino

University of Maryland, College Park, Maryland, USA
A. Baden, A. Belloni, J. Bistany-riebman, Y.M. Chen, S.C. Eno, N.J. Hadley, S. Jabeen, R.G. Kellogg, T. Koeth, B. Kronheim, Y. Lai, S. Lascio, A.C. Mignerey, S. Nabili, C. Palmer, C. Papageorgakis, M.M. Paranjpe, E. Popova[91], A. Shevelev, L. Wang, L. Zhang

Massachusetts Institute of Technology, Cambridge, Massachusetts, USA
J. Bendavid, I.A. Cali, P.c. Chou, M. D'Alfonso, J. Eysermans, C. Freer, G. Gomez-Ceballos, M. Goncharov, G. Grosso, P. Harris, D. Hoang, D. Kovalskyi, J. Krupa, L. Lavezzo, Y.-J. Lee, K. Long, C. Mcginn, A. Novak, M.I. Park,

C. Paus, C. Reissel, C. Roland, G. Roland, S. Rothman, G.S.F. Stephans, Z. Wang, B. Wyslouch, T. J. Yang

University of Minnesota, Minneapolis, Minnesota, USA
B. Crossman, B.M. Joshi, C. Kapsiak, M. Krohn, D. Mahon, J. Mans, B. Marzocchi, M. Revering, R. Rusack, R. Saradhy, N. Strobbe

University of Nebraska-Lincoln, Lincoln, Nebraska, USA
K. Bloom, D.R. Claes, G. Haza, J. Hossain, C. Joo, I. Kravchenko, A. Rohilla, J.E. Siado, W. Tabb, A. Vagnerini, A. Wightman, F. Yan, D. Yu

State University of New York at Buffalo, Buffalo, New York, USA
H. Bandyopadhyay, L. Hay, H.w. Hsia, I. Iashvili, A. Kalogeropoulos, A. Kharchilava, M. Morris, D. Nguyen, S. Rappoccio, H. Rejeb Sfar, A. Williams, P. Young

Northeastern University, Boston, Massachusetts, USA
G. Alverson, E. Barberis, J. Bonilla, B. Bylsma, M. Campana, J. Dervan, Y. Haddad, Y. Han, I. Israr, A. Krishna, J. Li, M. Lu, R. Mccarthy, D.M. Morse, V. Nguyen, T. Orimoto, A. Parker, L. Skinnari, E. Tsai, D. Wood

Northwestern University, Evanston, Illinois, USA
J. Bueghly, S. Dittmer, K.A. Hahn, D. Li, Y. Liu, M. Mcginnis, Y. Miao, D.G. Monk, M.H. Schmitt, A. Taliercio, M. Velasco

University of Notre Dame, Notre Dame, Indiana, USA
G. Agarwal, R. Band, R. Bucci, S. Castells, A. Das, R. Goldouzian, M. Hildreth, K. Hurtado Anampa, T. Ivanov, C. Jessop, K. Lannon, J. Lawrence, N. Loukas, L. Lutton, J. Mariano, N. Marinelli, I. Mcalister, T. McCauley, C. Mcgrady, C. Moore, Y. Musienko[15], H. Nelson, M. Osherson, A. Piccinelli, R. Ruchti, A. Townsend, Y. Wan, M. Wayne, H. Yockey, M. Zarucki, L. Zygala

The Ohio State University, Columbus, Ohio, USA
A. Basnet, M. Carrigan, L.S. Durkin, C. Hill, M. Joyce, M. Nunez Ornelas, K. Wei, D.A. Wenzl, B.L. Winer, B. R. Yates

Princeton University, Princeton, New Jersey, USA
H. Bouchamaoui, K. Coldham, P. Das, G. Dezoort, P. Elmer, A. Frankenthal, B. Greenberg, N. Haubrich, K. Kennedy, G. Kopp, S. Kwan, D. Lange, A. Loeliger, D. Marlow, I. Ojalvo, J. Olsen, D. Stickland, C. Tully, L.H. Vage

University of Puerto Rico, Mayaguez, Puerto Rico, USA
S. Malik, R. Sharma

Purdue University, West Lafayette, Indiana, USA
A.S. Bakshi, S. Chandra, R. Chawla, A. Gu, L. Gutay, M. Jones, A.W. Jung, A.M. Koshy, M. Liu, G. Negro, N. Neumeister, G. Paspalaki, S. Piperov, V. Scheurer, J.F. Schulte, M. Stojanovic, J. Thieman, A. K. Virdi, F. Wang, A. Wildridge, W. Xie, Y. Yao

Purdue University Northwest, Hammond, Indiana, USA
J. Dolen, N. Parashar, A. Pathak

Rice University, Houston, Texas, USA
D. Acosta, A. Agrawal, T. Carnahan, K.M. Ecklund, P.J. Fernández Manteca,

S. Freed, P. Gardner, F.J.M. Geurts, I. Krommydas, W. Li, J. Lin, O. Miguel Colin, B.P. Padley, R. Redjimi, J. Rotter, E. Yigitbasi, Y. Zhang

University of Rochester, Rochester, New York, USA
A. Bodek, P. de Barbaro, R. Demina, J.L. Dulemba, A. Garcia-Bellido, O. Hindrichs, A. Khukhunaishvili, N. Parmar, P. Parygin[91], R. Taus

Rutgers, The State University of New Jersey, Piscataway, New Jersey, USA
B. Chiarito, J.P. Chou, S.V. Clark, D. Gadkari, Y. Gershtein, E. Halkiadakis, M. Heindl, C. Houghton, D. Jaroslawski, S. Konstantinou, I. Laflotte, A. Lath, R. Montalvo, K. Nash, J. Reichert, P. Saha, S. Salur, S. Schnetzer, S. Somalwar, R. Stone, S.A. Thayil, S. Thomas, J. Vora

University of Tennessee, Knoxville, Tennessee, USA
D. Ally, A.G. Delannoy, S. Fiorendi, S. Higginbotham, T. Holmes, A.R. Kanuganti, N. Karunarathna, L. Lee, E. Nibigira, S. Spanier

Texas A&M University, College Station, Texas, USA
D. Aebi, M. Ahmad, T. Akhter, K. Androsov[60], O. Bouhali[92], R. Eusebi, J. Gilmore, T. Huang, T. Kamon[93], H. Kim, S. Luo, R. Mueller, D. Overton, A. Safonov

Texas Tech University, Lubbock, Texas, USA
N. Akchurin, J. Damgov, N. Gogate, A. Hussain, Y. Kazhykarim, K. Lamichhane, S.W. Lee, A. Mankel, T. Peltola, I. Volobouev

Vanderbilt University, Nashville, Tennessee, USA
E. Appelt, Y. Chen, S. Greene, A. Gurrola, W. Johns, R. Kunnawalkam Elayavalli, A. Melo, D. Rathjens, F. Romeo, P. Sheldon, S. Tuo, J. Velkovska, J. Viinikainen

University of Virginia, Charlottesville, Virginia, USA
B. Cardwell, H. Chung, B. Cox, J. Hakala, R. Hirosky, A. Ledovskoy, C. Mantilla, C. Neu

Wayne State University, Detroit, Michigan, USA
S. Bhattacharya, P.E. Karchin

University of Wisconsin - Madison, Madison, Wisconsin, USA
A. Aravind, S. Banerjee, K. Black, T. Bose, E. Chavez, S. Dasu, P. Everaerts, C. Galloni, H. He, M. Herndon, A. Herve, C.K. Koraka, A. Lanaro, R. Loveless, J. Madhusudanan Sreekala, A. Mallampalli, A. Mohammadi, S. Mondal, G. Parida, L. Pétré, D. Pinna, A. Savin, V. Shang, V. Sharma, W.H. Smith, D. Teague, H.F. Tsoi, W. Vetens, A. Warden

Authors affiliated with an international laboratory covered by a cooperation agreement with CERN
S. Afanasiev, V. Alexakhin, D. Budkouski, I. Golutvin†, I. Gorbunov, V. Karjavine, O. Kodolova[94], V. Korenkov, A. Lanev, A. Malakhov, V. Matveev[95], A. Nikitenko[96,94], V. Palichik, V. Perelygin, M. Savina, V. Shalaev, S. Shmatov, S. Shulha, V. Smirnov, O. Teryaev, N. Voytishin, B.S. Yuldashev[97], A. Zarubin, I. Zhizhin

Authors affiliated with an institute formerly covered by a cooperation agreement with CERN
G. Gavrilov, V. Golovtcov, Y. Ivanov, V. Kim[95], P. Levchenko[98], V. Murzin, V. Oreshkin, D. Sosnov, V. Sulimov, L. Uvarov, A. Vorobyev†, Yu. Andreev,

A. Dermenev, S. Gninenko, N. Golubev, A. Karneyeu, D. Kirpichnikov, M. Kirsanov, N. Krasnikov, I. Tlisova, A. Toropin, T. Aushev, K. Ivanov, V. Gavrilov, N. Lychkovskaya, V. Popov, A. Zhokin, M. Chadeeva[95], R. Chistov[95], S. Polikarpov[95], V. Andreev, M. Azarkin, M. Kirakosyan, A. Terkulov, E. Boos, V. Bunichev, M. Dubinin[83], L. Dudko, A. Gribushin, V. Klyukhin, S. Obraztsov, M. Perfilov, V. Savrin, P. Volkov, G. Vorotnikov, V. Blinov[95], T. Dimova[95], A. Kozyrev[95], O. Radchenko[95], Y. Skovpen[95], V. Kachanov, S. Slabospitskii, A. Uzunian, A. Babaev, V. Borshch, D. Druzhkin

†: Deceased
[1]Also at Yerevan State University, Yerevan, Armenia
[2]Also at TU Wien, Vienna, Austria
[3]Also at Ghent University, Ghent, Belgium
[4]Also at Universidade do Estado do Rio de Janeiro, Rio de Janeiro, Brazil
[5]Also at FACAMP - Faculdades de Campinas, Sao Paulo, Brazil
[6]Also at Universidade Estadual de Campinas, Campinas, Brazil
[7]Also at Federal University of Rio Grande do Sul, Porto Alegre, Brazil
[8]Also at University of Chinese Academy of Sciences, Beijing, China
[9]Also at China Center of Advanced Science and Technology, Beijing, China
[10]Also at University of Chinese Academy of Sciences, Beijing, China
[11]Also at China Spallation Neutron Source, Guangdong, China
[12]Now at Henan Normal University, Xinxiang, China
[13]Also at University of Shanghai for Science and Technology, Shanghai, China
[14]Now at The University of Iowa, Iowa City, Iowa, USA
[15]Also at an institute formerly covered by a cooperation agreement with CERN
[16]Also at Cairo University, Cairo, Egypt
[17]Also at Suez University, Suez, Egypt
[18]Now at British University in Egypt, Cairo, Egypt
[19]Also at Purdue University, West Lafayette, Indiana, USA
[20]Also at Université de Haute Alsace, Mulhouse, France
[21]Also at Istinye University, Istanbul, Turkey
[22]Also at The University of the State of Amazonas, Manaus, Brazil
[23]Also at University of Hamburg, Hamburg, Germany
[24]Also at RWTH Aachen University, III. Physikalisches Institut A, Aachen, Germany
[25]Also at Bergische University Wuppertal (BUW), Wuppertal, Germany
[26]Also at Brandenburg University of Technology, Cottbus, Germany
[27]Also at Forschungszentrum Jülich, Juelich, Germany
[28]Also at CERN, European Organization for Nuclear Research, Geneva, Switzerland
[29]Also at HUN-REN ATOMKI - Institute of Nuclear Research, Debrecen, Hungary
[30]Now at Universitatea Babes-Bolyai - Facultatea de Fizica, Cluj-Napoca, Romania
[31]Also at MTA-ELTE Lendület CMS Particle and Nuclear Physics Group, Eötvös Loránd University, Budapest, Hungary
[32]Also at HUN-REN Wigner Research Centre for Physics, Budapest, Hungary
[33]Also at Physics Department, Faculty of Science, Assiut University, Assiut, Egypt
[34]Also at Punjab Agricultural University, Ludhiana, India
[35]Also at University of Visva-Bharati, Santiniketan, India
[36]Also at Indian Institute of Science (IISc), Bangalore, India
[37]Also at Amity University Uttar Pradesh, Noida, India
[38]Also at IIT Bhubaneswar, Bhubaneswar, India
[39]Also at Institute of Physics, Bhubaneswar, India

[40]Also at University of Hyderabad, Hyderabad, India
[41]Also at Deutsches Elektronen-Synchrotron, Hamburg, Germany
[42]Also at Isfahan University of Technology, Isfahan, Iran
[43]Also at Sharif University of Technology, Tehran, Iran
[44]Also at Department of Physics, University of Science and Technology of Mazandaran, Behshahr, Iran
[45]Also at Department of Physics, Faculty of Science, Arak University, ARAK, Iran
[46]Also at Helwan University, Cairo, Egypt
[47]Also at Italian National Agency for New Technologies, Energy and Sustainable Economic Development, Bologna, Italy
[48]Also at Centro Siciliano di Fisica Nucleare e di Struttura Della Materia, Catania, Italy
[49]Also at Università degli Studi Guglielmo Marconi, Roma, Italy
[50]Also at Scuola Superiore Meridionale, Università di Napoli 'Federico II', Napoli, Italy
[51]Also at Fermi National Accelerator Laboratory, Batavia, Illinois, USA
[52]Also at Lulea University of Technology, Lulea, Sweden
[53]Also at Consiglio Nazionale delle Ricerche - Istituto Officina dei Materiali, Perugia, Italy
[54]Also at Institut de Physique des 2 Infinis de Lyon (IP2I), Villeurbanne, France
[55]Also at Department of Applied Physics, Faculty of Science and Technology, Universiti Kebangsaan Malaysia, Bangi, Malaysia
[56]Also at Consejo Nacional de Ciencia y Tecnología, Mexico City, Mexico
[57]Also at Trincomalee Campus, Eastern University, Sri Lanka, Nilaveli, Sri Lanka
[58]Also at Saegis Campus, Nugegoda, Sri Lanka
[59]Also at National and Kapodistrian University of Athens, Athens, Greece
[60]Also at Ecole Polytechnique Fédérale Lausanne, Lausanne, Switzerland
[61]Also at Universität Zürich, Zurich, Switzerland
[62]Also at Stefan Meyer Institute for Subatomic Physics, Vienna, Austria
[63]Also at Laboratoire d'Annecy-le-Vieux de Physique des Particules, IN2P3-CNRS, Annecy-le-Vieux, France
[64]Also at Near East University, Research Center of Experimental Health Science, Mersin, Turkey
[65]Also at Konya Technical University, Konya, Turkey
[66]Also at Izmir Bakircay University, Izmir, Turkey
[67]Also at Adiyaman University, Adiyaman, Turkey
[68]Also at Bozok Universitetesi Rektörlügü, Yozgat, Turkey
[69]Also at Marmara University, Istanbul, Turkey
[70]Also at Milli Savunma University, Istanbul, Turkey
[71]Also at Kafkas University, Kars, Turkey
[72]Now at Istanbul Okan University, Istanbul, Turkey
[73]Also at Hacettepe University, Ankara, Turkey
[74]Also at Erzincan Binali Yildirim University, Erzincan, Turkey
[75]Also at Istanbul University - Cerrahpasa, Faculty of Engineering, Istanbul, Turkey
[76]Also at Yildiz Technical University, Istanbul, Turkey
[77]Also at School of Physics and Astronomy, University of Southampton, Southampton, United Kingdom
[78]Also at IPPP Durham University, Durham, United Kingdom
[79]Also at Monash University, Faculty of Science, Clayton, Australia
[80]Also at Università di Torino, Torino, Italy
[81]Also at Bethel University, St. Paul, Minnesota, USA
[82]Also at Karamanoğlu Mehmetbey University, Karaman, Turkey

[83]Also at California Institute of Technology, Pasadena, California, USA
[84]Also at United States Naval Academy, Annapolis, Maryland, USA
[85]Also at Ain Shams University, Cairo, Egypt
[86]Also at Bingol University, Bingol, Turkey
[87]Also at Georgian Technical University, Tbilisi, Georgia
[88]Also at Sinop University, Sinop, Turkey
[89]Also at Erciyes University, Kayseri, Turkey
[90]Also at Horia Hulubei National Institute of Physics and Nuclear Engineering (IFIN-HH), Bucharest, Romania
[91]Now at another institute formerly covered by a cooperation agreement with CERN
[92]Also at Texas A&M University at Qatar, Doha, Qatar
[93]Also at Kyungpook National University, Daegu, Korea
[94]Also at Yerevan Physics Institute, Yerevan, Armenia
[95]Also at another institute formerly covered by a cooperation agreement with CERN
[96]Also at Imperial College, London, United Kingdom
[97]Also at Institute of Nuclear Physics of the Uzbekistan Academy of Sciences, Tashkent, Uzbekistan
[98]Also at Northeastern University, Boston, Massachusetts, USA